WAVE TRANSMISSION OVER ARTIFICIAL REEFS

A Physical Model Study

L. Buis

WAVE TRANSMISSION OVER ARTIFICIAL REEFS

A PHYSICAL MODEL STUDY

Master Thesis

To obtain the degree of master of science at the Delft University of Technology

by

LISANNE BUIS

Student number: 4469682
Thesis committee: Prof. dr. ir. M. R. A. van Gent,   TU Delft, Deltares (Chair)
                    Dr. ir. D. Wüthrich,   TU Delft
                    Ir. J. P. van den Bos,   TU Delft, Boskalis

PREFACE

Before you lies my thesis, which marks the end of my years as a student at Delft University of Technology.

As a civil engineering student, I was drawn in by the tangibility of the subject, and the fact that it can be seen in our surroundings every day. This is also the reason I wanted to work on a physical model during my thesis project. I am happy that Marcel van Gent gave me the opportunity to conduct experiments at the wave flume of Deltares. The combination of the practical work and the ability to make a contribution to the knowledge space of the functioning of artificial as coastal breakwaters, sparked my interest in this subject.

First, I would like to thank my graduation committee: Marcel van Gent who is the chair and also my daily supervisor. You were easily accessible for a discussion and provided me with useful feedback, which I really appreciated. Thank you Davide Wüthrich for your genuine involvement and extensive feedback, and thank you Jeroen van den Bos for all your ideas and advice from more a practical point of view. I felt comfortable with you as a committee and always had the feeling I could ask you any question. Moreover, I would like to thank all my Deltares colleagues from the Coastal Structures department for all the nice coffee breaks and lunches. Thanks to my friends from civil engineering for all the coffee breaks at the faculty during our graduation projects. This made studying during the summer days more fun!

A warm thanks to my housemates. First, my housemates in Delft. I value how we were not only housemates, but also became friends that I believe will never lose sight of each other. Special thanks to Annabel, I appreciate the time you took to point out all the grammar mistakes and missing commas in my thesis. During my thesis, I moved to Rotterdam. I want to thank my new housemates for creating a new comfortable home here.

And lastly, a warm thanks to my family. My parents for their unconditional support, not only supporting me in my study, but also in all my sports ambitions. And my brothers, who definitely did not share my interest in mathematics and physics but always admired what I did here in Delft.

Enjoy reading!

Lisanne Buis
Rotterdam, September 2022

SUMMARY

Currently, 70% of the sandy coasts in the world experience erosion. Simultaneously, the biodiversity in the oceans is decreasing. Coral reefs play an important role in protecting coasts as they provide a sheltered habitat for marine life and absorb wave energy in the foreshore. Therefore, they are essential for the preservation of the biodiversity in the oceans and morphology of the coastlines. However, already 60% of the coral reefs is nowadays under threat, because of a combination of ocean warming, acidification, and other anthropogenic impacts. In the next 50 years, the hydraulic conditions in which coral reefs have lived in the past centuries will be exceeded. Moreover, since it takes 15 to 25 years for coral reefs to recover from destructing events, they might disappear completely in the future. This can have serious consequences for the biodiversity in the oceans and erosion of the coastlines.

In response to this threat, various artificial reefs are being designed. However, as artificial reefs are all very different in design, it is difficult to quantify the functioning of artificial reefs as a coastal breakwater. As it is not realistic to test every artificial reef on its wave transmission, a more fundamental approach to identifying the effect of artificial reefs on the wave transmission is needed. This leads to the following research question that will be answered in this thesis: *How do the permeability and the porosity of an artificial coastal reef influence wave transmission and the sheltered habitat of marine life?* A physical model is used to answer this question.

In the physical model, five trapezoidal breakwaters are tested. One breakwater was impermeable, one was a rubble mound breakwater, and three breakwaters were hollow with a perforated outer surface. Thus, the permeability and (surface) porosity were varied. It was concluded that the volume porosity is of great influence on the wave transmission since the hollow perforated breakwater showed very different wave transmissions than the rubble mound breakwater with an identical surface porosity. However, similar wave transmissions as for a smooth impermeable and rubble mound breakwater were measured when a vertical impermeable screen was positioned inside this hollow perforated structure. From this, it was concluded that the permeability of the vertical screen determines the wave transmission.

Moreover, it was concluded that the smooth impermeable breakwater showed mostly lower wave transmissions than the rubble mound breakwater. This shows that the wave dissipation due to more severe wave breaking for impermeable structures is stronger than the dissipation due to roughness and friction inside the structure for permeable structures.

As the smooth impermeable, rubble mound, and hollow perforated breakwater with an impermeable screen showed similar wave transmissions, a new empirical relation was derived. This relation takes into account the relative crest freeboard and the relative

structure height. This new empirical relation is an improvement on existing empirical relations.

For the measured velocities inside the structures, a clear correlation between the velocity and wave height and wave length was observed only in the hollow perforated breakwater with an impermeable screen. Therefore, only this breakwater has been analysed. From the measured velocities it was concluded that the structure reduces the horizontal orbital velocity inside the structure. Remarkable is that the highest velocities measured in the structure, are on the lee side of the impermeable screen and in offshore direction. This is probably caused by the formation of an eddy in the shadow zone of the impermeable screen. The velocities were low enough for marine life to find shelter during the tested storm conditions and therefore, it could function as an artificial reef besides its function as a coastal breakwater.

Moreover, the transmitted wave spectrum of the breakwaters has been investigated. From this, it was concluded that hollow perforated structures (also with a perforated screen) transmit mostly longer waves. Whereas the smooth impermeable, rubble mound, and perforated structure with an impermeable screen, transmit mostly shorter waves. For these last structures also a cut in the higher frequencies was observed. From this it was concluded that a cut in higher frequencies is not only caused by the flow *through* the breakwater, but also caused by the *permeability* of the screen.

This newly obtained knowledge could affect the future design of artificial reefs. The main finding of this research is that a hollow, perforated structure can act as both an artificial reef that provides a safe habitat for marine life, and as a breakwater that provides sufficient coastal protection. This research therefore gives artificial reef designers the freedom to focus more on the ecological aspects of the structure, as its proper functioning as a breakwater can now be quantified and guaranteed when an impermeable screen is placed inside the artificial reef.

CONTENTS

LIST OF FIGURES

LIST OF TABLES

LIST OF SYMBOLS

Symbol	Unit	Discription
ν_k	m^2/s	kinematic viscoity
λ	-	scale factor
ω	rad/s	angular frequency
ρ_w	kg/m^3	water density
σ	kg^2	surface tension
$\tan\alpha$	rad	seaward slope of structure
$\xi_{0,p}$	-	breaker parameter
a	m	wave amplitude
B_c	m	crest width
d	m	water depth
D_{n50}	m	nominal diameter
Fr	-	Froude number
g	m/s^2	gravitational acceleration
h	m	structure height
$H_s i$	m	incident significant wave height
$H_s t$	m	transmitted significant wave height
H_{m0}	m	significant wave height
k	-	wave number
K_t	-	wave transmission coefficient
L	m	wave length
n	-	porosity
R_c	m	crest freeboard
Re	-	Reynolds number
s	-	wave steepness
T_p	s	peak period
$T_{m-1,0}$	s	mean energy wave period
u	m/s	water velocity
We	-	Weber number
$\hat{u}_x$	m/s	particle horizontal orbital velocity

1

INTRODUCTION

The coastline is defined as the boundary between sea and land. The coastline is highly dynamic as it is constantly shifting due to changes in the hydraulic forces and natural environment. As a consequence of these changes in the last decades, at the moment 70% of the sandy coasts in the world experience erosion (Yincan et al, 2017). As 37% of the global population that lives in coastal communities is dependent on the oceans, coastal, and marine resources, engineers are constantly battling coastal erosion (United Nations, 2017).

Moreover, the biodiversity in the oceans is decreasing. 60% of the coral reefs nowadays is under threat by a combination of ocean warming, acidification and other anthropogenic impacts (Hoegh-Guldeberg, 2010). Coral reefs are essential for the preservation of biodiversity as they provide a sheltered habitat for marine life. However, in the next 50 years, the hydraulic conditions in which the coral reefs have lived in the past centuries will be exceeded (T. P. Hughes et al., 2003). Already, 40-50% less coral cover than 30 years ago is observed, due to global warming and human interference such as over-exploitation of key species and destructive fishing practices ((Hoegh-Guldeberg, 2010); (T. P. Hughes et al., 1996); (T. P. Hughes et al., 2003)). As it takes 15-25 years for coral reefs to recover, they may disappear completely in the future. In Figure 1.1, the changes on coral reefs due to the warming of seas associated with a doubling of carbon dioxide over pre-industrial levels, 560 ppm by 2100, are projected.
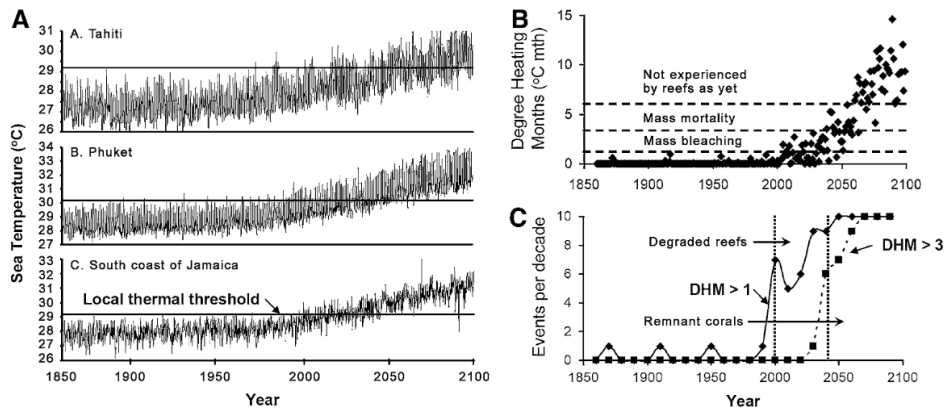
Figure 1.1: Projections of change on coral reefs due to the warming of seas associated with a doubling of carbon dioxide over pre-industrial levels (Hoegh-Guldeberg, 2010). A: Sea surface temperature data for Tahiti, Thailand, and Jamaica conform to IPCC scenario IS92a. Above the local thermal threshold bleaching begins. B: Degree Heating Months (DHM = Anomaly above thermal tolerance treshold exposure x exposure time in months) calculated for the climate modeling data shown in A. DHM 1-3 causes bleaching, DHM 3- 5 causes mass mortality. Values higher than 6 have not been seen on reefs yet. C: Frequency of bleaching events and mass mortality events.

1.1. PROBLEM STATEMENT

In response to this threat, various artificial coastal reefs are being designed. Artificial reefs are defined as solid man-made structures that have been submerged in the natural environment (Bohnsack, 1998). Some artificial reefs are Lego-like structures, porous blocks stacked onto each other. Other artificial reefs are individual structures grouped together at the foreshore. The primary aim of these artificial reefs is to create a sheltered habitat for marine life. Subsequently, these artificial reefs could function as a submerged breakwater to decrease coastal erosion.

However, quantifying the function of artificial reefs as coastal breakwater is still difficult as they are all very different in design. Current empirical relations for the wave transmission developed by for instance van der Meer (1990) and d'Angremond et al. (1996) are primarily based on physical models with conventional breakwaters. For some artificial reefs specific empirical relations are developed. However, it is unrealistic to test every new developed artificial reef in a wave flume to determine its wave transmission. Therefore, a more fundamental approach in identifying the effect of porosity and permeability on the wave transmission over artificial reefs is needed.

The aim of this thesis is to provide more insight into the parameters *permeability* and *porosity*, affecting the wave transmission over artificial reefs. With this knowledge, the design of artificial reefs functioning as coastal breakwater could be improved. Moreover, the influence of the permeability and porosity on the velocities inside the artificial reefs is investigated to still enhance a sheltered habitat for marine life.

1.2. RESEARCH QUESTIONS

The main research question that will be answered in this thesis is:

> How do the permeability and the porosity of an artificial coastal reef influence wave transmission and the sheltered habitat of marine life?

This research question is split into sub-questions and a physical model will be used to obtain the knowledge needed to answer these questions.

- How can experiments in a flume be designed to obtain knowledge about the influence of permeability and porosity on the wave transmission and velocities inside the structure of an artificial reef?

- What are the results of the physical model tests and how can they be interpreted?

    (a) What are the measured wave transmissions from the physical model?

    (b) What is the influence of the relative crest freeboard (R_c/H_s), relative structure height (h/H_s), and wave steepness (H_s/L) on the wave transmission (K_t)?

    (c) What is the influence of an artificial reef on the horizontal orbital velocities inside the structure?

- How do the measured wave transmissions from the physical model relate to the existing empirical relations?

- Can a new empirical relation for the wave transmission over artificial coastal reefs be derived from the physical model results?

1.3. RESEARCH METHODOLOGY AND SCOPE

In this section the research methodology used to answer the previously stated research questions will be explained. This methodology is divided into three parts: literature study, physical model, and data analysis. Moreover, the scope of the research is defined.

Literature Study   In the literature study, the required existing knowledge on the functioning of breakwaters and artificial reefs is obtained. The literature study is divided in two parts. The first part covers coral reefs, knowledge about the marine life and current artificial reefs is obtained here. The second part covers breakwaters. Here, the current available knowledge and relations on the wave transmission is obtained.

Physical Model   A physical model is used to obtain the required data that is needed to answer the research questions. A physical model is used to predict physical phenomena from the real world in a down-scaled environment which can not be accurately simulated with numerical models. For this physical model, a two-dimensional flume at Deltares is used. Scaling laws are used to guarantee representativity between the model and the prototype. In 4 weeks time, 208 tests were performed to obtain the required data on wave transmission and water velocities.

Data Analysis   In this part of the research, the obtained results from the physical model will be interpreted. For this, the knowledge gained in the literature study is used to compare the results to existing empirical relations. Python Notebook is used to analyse and plot the data. Following from this data analysis, the remaining answers to the research questions are found. Finally, this leads to the answer on the main research question.

Although the research has an ecological interest, the ecological function of artificial reefs will be considered out of scope. However, some hydraulic boundary conditions will be assumed from which it is known that certain organisms can survive. In this way, also the ecological value can be indirectly considered. Moreover, only the wave-induced forces and velocities are investigated. In reality, side-specific forces will be present at the artificial reef too, such as oceanic currents. As for this research, the interest lies primarily with storm conditions. Other processes, such as oceanographic currents, can be neglected. Lastly, only normal incident waves are tested, obliquely incident waves are left out of scope for this research.

1.4. READING GUIDE

- *2. Literature Review*: In chapter 2, a literature study is performed to gain insight into the development of coral reefs and the function of a submerged breakwater.

- *3. Physical Model*: In chapter 3, the physical model that is used to find the answer to the main research question is elaborated upon. In this section, the scaling of the model, the experimental setup in the flume, and the performed runs are discussed.

- *4. Data Analysis*: In chapter 4, the data analysis that is performed using the data of the conducted experiments is discussed. First, the results from the measured wave transmissions are analysed. Consecutively, the wave spectrum, and orbital velocities measured inside the breakwaters are elaborated upon.

- *5. Discussion*: In chapter 5, the discussion points and main limitations of this research will be discussed.

- *6. Conclusion and Recommendations*: In chapter 6, the conclusions from the research are made. This includes the answers to the (sub-) research questions that were previously stated. Also, some recommendations for further research are proposed.

2

LITERATURE REVIEW

In this chapter, a literature study is performed to gain insight into the development of coral reefs and the functioning of a submerged breakwater. First, the factors influencing the development of coral reefs is investigated. This is followed by examples of artificial reefs that are designed nowadays. Thereafter, the marine life which lives in coral reefs are investigated. Next, submerged breakwaters are elaborated upon, followed by the already existing empirical relations for wave transmission.

2.1. CORAL REEFS

Coral reefs are mainly found in regions within 30 degrees north or south of the equator, as the water temperature must not be lower than 18 degrees (Hoegh-Guldeberg, 2010). Because of their need for abundant light, they grow in shallow seas and avoid areas where turbidity from the sediment transport of rivers is present (Hoegh-Guldeberg, 2010). Another factor that is important for the development of coral reefs is the concentration of carbonate ions, which is dependent on the acidity of the ocean. This, in turn, follows from the carbon dioxide concentration in the atmosphere (Hoegh-Guldeberg, 2010). The degree of saturation is mostly influenced by the temperature and decreases towards the poles. This means that coral reefs are mostly found in shallow equatorial coastal regions that are warm, sunlit, and saturated with carbonate ions.

The events that are threatening these conditions nowadays are sea-level rise, global warming, storm intensity and frequency, and acidification. The impacts of these events are briefly explained:

- **Sea-Level Rise** - A feature of coral reefs is that they can grow with the sea-level rise (SLR). However, if SLR goes too fast, the coral reefs will not be able to keep up. As a result, the light intrusion will be affected as the coral reef will receive less light for photosynthesis, which will accelerate the calcification rate of corals. Furthermore, the SLR will impact the hydrodynamics as the water depth above the reef is increased. This impacts the flow velocities and wave-breaking above the coral reef. This will result in higher hydraulic forces and pressures.

- **Global Warming** - The thermal conditions highly influence the development of coral reefs. As the temperature of the water increases, some coral reefs will not be able to survive (Hoegh-Guldberg et al., 2007)

- **Storm intensity and frequency** - Due to climate change, the intensity and frequency of storms can increase. This results in higher hydraulic loadings on the reef structure which could lead to severe damage. It may take 15-20 years for coral reefs to recover from such an impact. So if in that time too many storms occur, the coral reefs may disappear completely.

- **Acidification** - With the increase in CO_2 concentration in the atmosphere, the pH of the water is also affected. This negatively influences the calcification of corals and thereby their growth. The increase in CO_2 concentration in the ocean is called acidification.

There are also cold-water coral reefs. These reefs do not need light to survive and can be found in deeper depths. You can find cold coral reefs at depths of 40 to 1000 meters with temperatures as low as 4 degrees (WWF, 2004). Due to their basic lifestyle, they are extremely vulnerable. Any change in their hydraulic environment could result in damage. Therefore you will only find them in environments which have low and stable hydraulic forces. Moreover, they develop slowly, so if any damage occurred, it could take up to a hundred years to rebuild (WWF, 2004). As a result, these coral reefs will not be found in the nearshore where they could function as a wave energy absorber.

2.1.1. Artificial Reefs

Artificial reefs can be defined as solid, man-made structures that have been submerged in the natural environment (Bohnsack, 1998). These reefs are often called low-crested structures (LCS). Artificial reefs are used primarily for habitat restoration and beach erosion control (Cardenas-Rojas et al., 2021). The succes of these artifical reefs to fulfil this function depends on: hydrodamic, morphological, and ecological performance.

Hydrodynamic performance   The hydrodynamic performance of an artificial reef is the extent to which the reef reduces the energy of the waves that attack the beach. The goal of the structure is to have a low transmission coefficient, which is the proportion of waves on the protected side with respect to the waves before the structure. When waves interact with an obstacle, the energy transformation following from the energy law is breakage, steepening, reflection, and dissipation. Submerged structures that have a low water depth above the crest of the breakwater will cause breakage of a high percentage of the waves which leads to more dissipation of energy. Moreover, structures that are low in porosity will create greater reflection. When the water depth above the structure is large, it can happen that the waves propagate over the structure and do not break. The wave height could even slightly increase do to shoaling that is caused by the breakwater (Cardenas-Rojas et al., 2021). The height of the structure, size, and its position to the shoreline determine the coastal protection level (Pilarczyk, 2003).

Morphological performance   The morphological performance of an artificial reef is its effect on the beach profile and sediment budget of the beach. The structure firstly serves as a trap for the cross-shore sediment transport (Ma et al., 2020). This function could be of use in areas where storms occur. Then the barrier is maintaining the beach as the sediment is trapped when a storm transports sediment from the beach offshore.

Moreover, the breaking at the crest of the structure creates a calm zone behind the structure. When extreme events occur and the sea level rises, the waves will break closer to the shore as they are able to propagate over the structure. Sediment that is trapped between the coast and the structure will then form bars which will contribute to the protection of the beach (Kuang et al., 2019).

Ecological Performance   The ecological performance of an artificial reef is its relation with ecosystems and marine organisms (Cardenas-Rojas et al., 2021). By constructing artificial reefs, the main ecological aspect that can be improved is the space inside the structure that can be colonised by a variety of marine species. Swimming organisms will be the first to find shelter and seek refuge inside the structure. From there, more diverse communities will develop, all depending on the characteristics of the site. Some species could even use it as a breeding area. Moreover, benthic colonisation will take place. With successful colonisation, there is a beginning of a succession process and a food chain. In some rare situation, this would include the growth of different coral species. Often it takes a maximum of up to 5 years for a community structure to achieve equilibrium after construction of the artificial reef (Bohnsack & Sutherland, 1985).

2.1.2. Examples of Artificial Reefs

The design of an artificial reef influences the marine life that it attracts (Lemoine et al., 2019). Important factors in the design are the volume, area and profile of a reef. Reefs with nearly vertical sides are considered to be the best because they increase turbulent flow, producing attractive sounds and creating stagnation zones and lee waves which attracts desired species of fish (Bohnsack & Sutherland, 1985). This is a good quality, as complexity is important for succesful artificial reefs.

Moreover, artificial reefs should be oriented perpendicular to prevailing currents and fish migratory pathways. Furthermore, spacing artificial reefs from 600 to 1000m from natural reefs is recommended to minimize fish interaction between reefs (Bohnsack & Sutherland, 1985). The effect of the artificial reefs on the species that it attracts is investigated by Lemoine et al. (2019). They concluded that concrete modules should be deployed if the objective is to mimic rocky reefs. Deploying ships will create habitats that are unlike natural reefs. However, it does creates fish abundance and biomass with different communities.

Below, some examples of artificial reefs will be discussed and visually presented in Figure 2.2.

MARS   Modular Artificial Reef Structure (MARS) is a ceramic 3D printed structure which is used for constructing a reef habitat without the need for heavy duty equipment. MARS can be deployed from small boats and implemented by divers. Each unit has a special surface geometry to encourage the development of juvenile coral. This 3D printed

and moulded ceramic is filled with marine concrete and steel reinforcement. Besides its function of transplanting coral, it also acts as habitat protection for other species in the area ("MARS — Reef Design Lab", n.d.).

MOSES   The MOdular SEalife System (MOSES) is a modular system to build artificial reefs ("MOSES / Solutions | ReefSystems", n.d.). These system modules serve as a habitat for aquatic animals to find food, shelter and a safe space to reproduce. Moreover, these reefs can also be installed as functional objects such as eco-anchors for floating solar panels or coastal erosion protection units. Blast furnace cement is used to reduce the CO_2 emission by 50% compared to traditional concrete.

Reef Balls   Reef balls are hollow, hemispherical-shaped artificial units primarily designed for the stimulation of biological growth and coral reef restoration. Besides, they could also function as coastal protection structures (Armono, 2004). A study has been performed to develop a model for wave transmission past a submerged breakwater constructed of multiple hemispherical-shaped artificial reef (HSAR) units. In Figure 2.1 the setup of the 5 different configurations that were tested are presented. Armono (2004) concluded that HSAR was able to dissipate on average approximately 60% of the incoming wave energy.
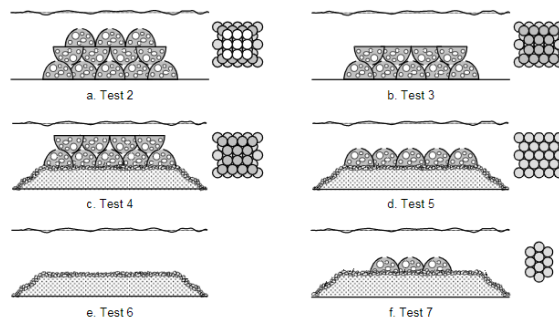
Figure 2.1: Test setup Reef Balls (Armono, 2004)

WABCORE   WAve Breaker COral REstoration (WABCORE) was developed by the National Hydraulics Research Institute Malaysia (NAHRIM). It consist of a prefabricated concrete structure stacked together for a simple trapezoidal design. For coral restoration WABCORE recorded a coral growth which increased from 8.66% to 29.75% on the whole surface of WABCORE in three years (Na'Im et al., 2018). Furthermore, from the physical model, 30% of the tests showed a wave dissipation of 50-75% and 40% showed a dissipation of 25-50% (Na'Im et al., 2018).

REB   The Reef Enhancing Breakwater (REB) is designed by Reefy and is a 'Lego-like' structure that consists of building blocks that were hydrodynamically designed and tested for stability. Through stacking and interlocking, these blocks can be assembled in different configurations to form a stable artificial reef that can dissipate over 90% of wave

energy. Also, a shelter for fish and invertebrate species is created. Therefore it provides coastal protection while the marine ecosystem can restore itself ("Eco-solutions – Reefy", n.d.).
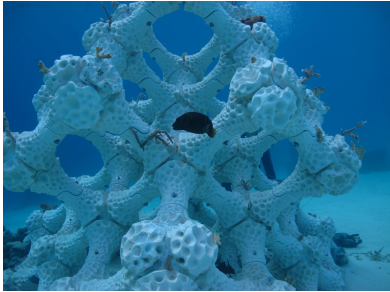
(a) MARS

(b) MOSES

(c) Reef Balls

(d) WABCORE

(e) REB

Figure 2.2: Examples of artificial reefs

2.1.3. Marine Life

In Table 2.1, an overview of the hydraulic boundary conditions for some marine life is presented (Profile et al., 2005). These conditions can be taken into account for the design of artificial reefs.

The feeding limit is the flow velocity needed to supply enough nutrients for the organisms. This flow velocity is mostly reached by the side specific oceanographic currents. The dislodgement and movement limits, are limits that might be exceeded during storm conditions. Hereby, movement is defined as some displacement but the organism is still attached or located in the reef. Dislodgement occurs when the organism gets fully detached of the reef.

Organism	Name	Streamwise Velocity u [m/s]
Barnacle	Belanus cretanis (a)	Growth optimum = 0.08 Movement limit: u >0.24
	Balanus glandula (b)	Feeding optimum u = 2-4
Sea urchin	Strongylocentrotus nudus (c)	Feeding limit: u >0.40 Movement limit: u >0.80
	Strongylocentrotus droebachienis (d) & Seastar: Asterias forbesi (e)	Dislodgement start : u >7
Mussel	Mytilus trossulus (f) & Mytilus edulis (g) (10-25 mm shell length)	Dislodgement start: u >7
Marine snail	Astraea undosa (h)	Dislodgement (50%): u >4

Table 2.1: Overview of hydrodynamic boundary organisms for certain marine life (Profile et al., 2005)

(a) Balanus cretanis, photo credit: Keith Hiscock

(b) Balanus glandula, photo credit: n.a.

(c) Strongylocentrotus nudus, photo credit: Totti

(d) Strongylocentrotus droebachienis, photo credit: Hannah Robinson

(e) Asterias forbesi, photo credit: Paul Morris

(f) Mytilus trossulus, photo credit: NNehring

(g) Mytilus edulis, photo credit: IMAGO / Nature Picture Library

(h) Astraea undosa, photo credit: Peter J. Bryant

Figure 2.3: Organisms in reefs

2.2. BREAKWATERS

As a secondary function, artificial reefs could act as a submerged breakwater. In this section, the function of traditional breakwaters will be elaborated upon. Moreover, the wave transmission over submerged breakwaters will be explained, together with its empirical solutions from previous research.

2.2.1. INTRODUCTION TO BREAKWATERS

Coastal protection has always been an essential challenge for engineers. Nowadays, they are challenged even more as also non-physical parameters are introduced to the problem, such as the environmental and aesthetic value of the nearshore landscape (Makris & Memos, 2007). Therefore, mild-type structures are preferred. Low-crested and submerged breakwaters are increasingly used as they are considered mild-type structures. Submerged breakwaters are designed to reduce the wave energy to protect the coasts against erosion or protect areas from waves (Sharif Ahmadian, 2016).

By decreasing the wave energy on the lee side of the structure, the sediment transport and the morphology of the coastal zone can be controlled. As the breakwater results in a decrease of the wave energy and turbulence behind the structure, this 'shadow zone' prevents the sediment from being transported with the return flow. The wave transmission over these structures is an important measure to identify the efficiency of the structure protecting the coast. The transmission coefficient is defined as the ratio between the transmitted and initial wave height.

The design of a submerged breakwater highly influences the wave transmission over the structure. In Figure 2.4, a sketch of a breakwater with its most important parameters according to van der Meer et al. (2005) is presented. Notice that these parameters are for emerged and submerged breakwaters. However, when only submerged breakwaters are considered some parameters such as the shape of the breakwater and roughness of the armour layer are considered to be of less influence on the wave transmission.
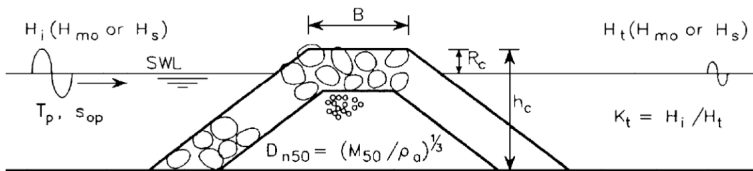
Figure 2.4: Definition of the governing parameters involved in wave transmission (van der Meer et al., 2005)

Where:

H_{si}	[m]	=	incident significant wave height
H_{st}	[m]	=	transmitted significant wave height
T_p	[s]	=	peak period
s_{op}		=	wave steepness, $s_{op} = 2\pi H_i / (g T_p^2)$
R_c	[m]	=	crest freeboard
h_c	[m]	=	structure height
B_c	[m]	=	crest width
D_{n50}	[m]	=	nominal diameter armour rock (rubble mound structure)
K_t		=	transmission coefficient, $\frac{H_t}{H_i}$
ξ_{op}		=	breaker parameter, $\xi_{op} = \frac{\tan\alpha}{s_{op}^{-1/2}}$
$\tan\alpha$	[rad]	=	seaward slope of structure

The wave transmission coefficient increases with submergence depth and wave period and decreases with raising the incident wave height and the breakwater crest width. Moreover, the seaside slope of the breakwater influences the energy for emerged conditions. Rock armour diameter and porosity can also play an important role in the dissipation of wave energy (van der Meer et al., 2005).

2.2.2. WAVE TRANSMISSION

As previously stated, the effect of a wave reducing construction is expressed by the wave transmission coefficient:

$$K_T = \sqrt{\frac{F_t}{F_i}} = \frac{H_{s,t}}{H_{s,i}} \tag{2.1}$$

where F_t and F_i are the energy flux. For irregular waves this can be expressed with the significant wave heights as a first approximation (Gerrit & Verhagen, 2016).

A number of laboratory tests has been performed to quantify these transmission coefficients. Following these data, empirical relations were derived. These formulas all come with their own limitations due to laboratory conditions and range of inputs. In Figure 2.5, an example of such an empirical relation is presented. From this figure it can be deducted that a breakwater can never completely reach a transmission coefficient of 0 or 1.
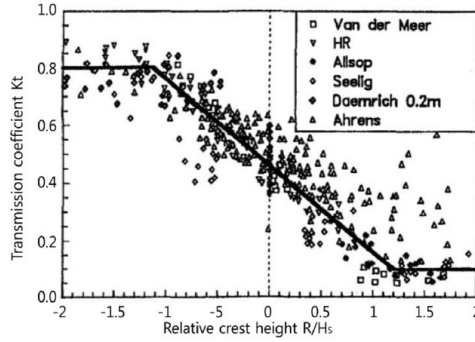
Figure 2.5: Wave transmission over a dam from d'Angremond et al., 1996

In general the wave transmission is influenced by the local wave characteristics, local bathymetry, design and placement pattern of the breakwater units, and the relative submergence. Previous researches have identified that the submerged depth (R_c/d) and crest width (B_c) are the critical and most important factors influencing the transmission process, while others have reported that the relative water depth (d/H_i), thickness-depth ratio (h/d) and relative freeboard (R_c/H_i) also contribute to wave transmission (Armono, 2004).

The empirical formula found by van der Meer (1990) in which K_t linearly depends on R_c/H_{si}, presented in Equation 2.2. Here K_t is only dependent on the incoming wave height and crest freeboard.

$$K_t = 0.46 - 0.3 \frac{R_c}{H_{si}} \tag{2.2}$$

An overview of the existing empirical relations are presented in Table 2.2. Below, these relations are elaborated upon.

- As a follow-up to the empirical relationship by van der Meer (1990), Daemen (1991) included the diameter of the armour rock, therefore the permeability of the armour layer was included. For a reef-type breakwater a different formula is defined as this shows different characteristics. Here the armour layer denotes a shallow structure made of a single layer of rock material.

- d'Angremond et al. (1996) made use of the work by Daemen (1991) and van der Meer (1990) and included the crest width in the formula. This made it possible to derive a formula for rubble mound and smooth structures. Here, for smooth impermeable breakwaters an almost identical formula was developed (now with a coefficient of 0.80 instead of 0.64). This formula only accounts for small crest widths. At that time, it was stated, using the limited available data, that rubble mound and smooth breakwaters respond more or less the same. Moreover, data from previous tests are filtered excluding high wave steepness's and breaking waves. Furthermore, structures that are highly submerged or emerged were excluded. Later, Briganti et al. (2003) developed a formula that is valid for wider crests as well.

- A physical model test for submerged breakwaters was executed by Seabrook and Hall (1998). Here, various values of the crest freeboard, crest width, water depth and incident wave conditions were applied. The formula from Seabrook and Hall (1998) is therefore restricted to submerged structures only.

- Bleck and Oumeraci (2001) designed a formula focusing on the energy transfer and local effects occurring at the reef. Here, the wave transmission is only dependent on the non-linearity parameter d/H_s.

- Calabrese et al. (2002) based their research on a large-scale test. The existing wave transmission formula has been verified and the influence of crest width and breaker index is highlighted. Later, Buccino and Calabrese (2007) formed a new prediction method for wave transmission based on simplified modelling of phenomena that rule wave energy transfer behind breakwaters, namely wave breaking, wave overtopping, and seepage through the body of barrier (Buccino & Calabrese, 2007).

- Friebel and Harris (2003) developed a best fit empirical model on data sets provided by Seelig (1980), Daemrich and Kahle (1985), van der Meer (1988) Daemen (1991) and Seabrook (1997). This study confirmed that the transmission coefficient is highly dependent on the non-dimensional freeboard R_c/H_{si}. To a lesser degree, the transmission coefficient also depends on the relative crest width B_c/L or B_c/h, on the relative structure emergence above sea bed $1 - R_c/h$, and on the ratio R_c/B_c.

- van der Meer et al. (2005) did a re-analysis on the research of d'Angremond et al. (1996) which led to a new equation for wave transmission at smooth low-crested breakwaters as it was observed that smooth and rubble mound breakwaters respond differently. van der Meer et al. (2005) reasoned that the wave transmission at smooth impermeable breakwaters is higher as there is no energy dissipation by friction and porosity of the breakwater. This is in contrast to the findings by Sollitt and Cross (1972) who observed that for a lower permeability the wave transmission reduces. Furthermore, it was stated that the crest width has less or no influence on the transmission as the smooth crest will not dissipate energy.

Author	Formula	Range of validity
Van der Meer, 1990	$K_t = 0.46 - 0.3 \frac{R_c}{H_{si}}$	$0.1 < K_t < 0.8$ $-1.13 < \frac{R_c}{H_{si}} < 1.2$
Daemen, 1991	$K_t = a \frac{R_c}{D_{n50}} + b$ $a = 0.031 \frac{H_{si}}{D_{n50}} - 0.24$ $b = -5.42 s_{0p} + 0.0323 \frac{H_{si}}{D_{n50}} + 0.51 - 0.017 \frac{B_c}{D_{n50}}^{1.84}$ *Reeftype* $K_t = a \frac{R_c}{D_{n50}} + b$ $a = 0.031 \frac{H_{si}}{D_{n50}} - 0.24$ $b = -2.6 s_{0p} - 0.05 \frac{H_{si}}{D_{n50}} + 0.85$	$0.075 < K_t < 0.75$ $-3 < R_c / D_{n50} < 5$ $1 < H_{si} / D_{n50} < 6$ $0.01 < s_{0p} < 0.05$ *Reeftype* $0.015 < K_t < 0.6$ $1 < H_{si} / D_{n50} < 6$ $0.01 < s_{0p} < 0.05$
d'Angremond et al. 1996	*Permeable* $K_t = -0.4 \frac{R_c}{H_{si}} + 0.64 \frac{B_c}{H_{si}}^{-0.31} (1 - e^{-0.5\xi})$ *Impermeable* $K_t = -0.4 \frac{R_c}{H_{si}} + 0.8 \frac{B_c}{H_{si}}^{-0.31} (1 - e^{-0.5\xi})$	$0.075 < Kt < 0.8$ $\frac{B_c}{H_{si}} < 10$
Seabrook & Hall 1998	$K_t = 1 - [e^{0.65 \frac{R_c}{H_{si}} - 1.09 \frac{H_{si}}{B_c}} - 0.047 \frac{B \cdot R_c}{L \cdot D_{n50}} + 0.067 \frac{R_c \cdot H_{si}}{B_c \cdot D_{n50}}]$	$-7.08 \leq \frac{B_c \cdot R_c}{L \cdot D_{n50}} \leq 0$ $-2.4 \leq \frac{R_c H_{si}}{B_c D_{n50}} \leq 0$
Bleck & Oumarci 2001	$K_t = 1 - 0.83 \cdot e^{-0.72 \frac{d_s}{H}}$	$\frac{B_c}{H_{si}} < 10$
Calabrese & Buccino 2002	$K_t = a \frac{R_c}{B_c} + b$ $a = (0.6957 \frac{H_{si}}{h_c} - 0.7021) \cdot e^{0.2568 \frac{B_c}{H_{si}}}$ $b = (1 - 0.562 e^{-0.0507\xi}) \cdot e^{|-0.0854 \frac{B_c}{H_{si}}|}$	$-0.4 \leq \frac{R_c}{B_c} \leq 0.3$ $1.06 \leq \frac{B}{H_{si}} \leq 8.13$ $0.31 \leq \frac{H_{si}}{h} \leq 0.61$ $3 \leq \xi_{0p} \leq 5.2$
Briganti et al. 2003	$K_t = -0.35 \frac{R_c}{H_{si}} + 0.51 (\frac{B_c}{H_{si}})^{-0.65} (1 - e^{-0.41\xi})$	$0.05 \leq K_t \leq 0.93 - 0.006 \frac{B_c}{H_{si}}$ $\frac{B_c}{H_{si}} > 10$
Friebel and Harris 2003	$K_t = -0.4969 \cdot e^{\frac{R_c}{H_{si}}} - 0.0292 \frac{B_c}{d_s} - 0.4257 \frac{h}{d_s} -$ $0.0696 \log \frac{B_c}{L} - 0.1359 \frac{R_c}{B_c} + 1.0905$	$-8.696 \leq R_c / H_{si} \leq 0$ $0.286 \leq B_c / d_s \leq 8.75$ $0.44 \leq h / d_s \leq 1$ $0.024 \leq B_c / L \leq 1.89$ $-1.050 \leq R_c / B_c \leq 0$
van der Meer et al. 2005	$Kt = -0.3 \frac{R_c}{H_{si}} + 0.75 \cdot [1 - \exp(-0.5\xi_{op})]$ $Kt = -0.3 \frac{R_c}{H_{si}} + [\frac{B}{H_{si}}]^{-0.31} \cdot [1 - \exp(-0.5\xi_{op})] \cdot 0.75$	For $\xi < 3$: For $\xi > 3$:
Buccino & Calabrese 2007	$K_t = (-1.18 (\frac{H_{si}}{R_c})^{0.12} - 0.33 (\frac{H_{si}}{R_c}^{1.5} \cdot \frac{B_c}{\sqrt{H_{si} \cdot L_{p0}}}))^{-1}$ $K_t = [min(0.74; 0.62 \cdot \xi_{0p}^{0.17}) - 0.25 \cdot min(2.2; \frac{B_c}{\sqrt{H_{si} \cdot L_{p0}}})]^2$	$-1/1.2 \geq \frac{R_c}{H_{si}} \geq -1/0.5$ $-1/1.2 \geq \frac{R_c}{H_{si}}$

Table 2.2: Overview empirical formulations wave transmission over breakwaters

The empirical relations from Table 2.2 are all considered for conventional breakwaters. However, for artificial reefs these relations may not suffice. Therefore, already some empirical relations have been developed for specific artificial reefs. Armono (2004) developed an empirical relation for the Reef balls, and Ibrahim et al. (2020) for WABCORE.

However, performing a physical test for every newly designed artificial reef is not realistic, therefore a more general approach for quantifying the wave transmission over artificial reefs is necessary.

2.2.3. POROSITY AND PERMEABILITY

In the empirical relations stated in the previous section, the permeability of the core, surface, and volume porosity are not taken into account so far. However, some physical model tests investigating the effects of permeability and porosity's of submerged breakwaters do have been performed.

Sollitt and Cross (1972) concluded that the transmission coefficient decreases with decreasing porosity and permeability. Permeability significantly affects the transmission, reflection, and dissipation of the wave energy. This is mainly due to the change of friction and wave breaking characteristics. Mahmoudi et al. (2017) stated that the wave transmission over an impermeable submerged breakwater is higher as there is no energy dissipation by friction and porosity of the structure which is opposite to the statements of Sollitt and Cross (1972).

Sidek et al. (2007) conducted a physical model with non-breaking wave transformation. From this, it is obtained that an increase in porosity resulted in an increase of the transmission coefficient. Moreover, the porous models were relatively less effective in dissipating wave energy against longer waves (lower kd values) compared to shorter waves (high kd values). Lokesha et al. (2019) investigated the effect of perforations on submerged artificial reefs for regular and random waves. Here, it was observed that an perforated breakwater with a surface porosity of 11% resulted in a small decrease of the wave transmission. This contradicts the findings of Koutandos et al. (2006). Probably there is a turning point from when the porosity results in extra wave dissipation or when the wave can just move through the structure without wave dissipation. Le Xuan et al. (2022) tested a hollow perforated emerged breakwater. This showed that the transmission coefficient depends on the breakwater porosity screen on both sides. The wave energy dissipation was highest when the porosity on the seaside is larger than on the shore side.

2.3. SUMMARY

Artificial reefs have two functions: one is to provide a sheltered habitat for marine life and one is to reduce the wave loads on the coastline. From section 2.1 it can be concluded that artificial reefs are very different in design. Testing every type of artificial coastal reef on its wave transmission does not seem realistic. However, it can be concluded from the previously discussed examples of artificial reefs that the permeability and porosity of the reefs differ greatly. Various researchers reached opposite conclusions about its effect on the wave transmission. Some concluded that increasing the permeability reduces the wave transmission while others concluded that increasing the

permeability increases the wave transmission. Identifying the effects of these variables on the wave transmission could already improve the knowledge about the functioning of artificial reefs as coastal protection.

In section 2.2 different empirical formulations for the wave transmission over submerged breakwaters are presented. Although, so far porosity and permeability effects are not taken into account, subsection 2.2.3 shows that there have been physical model tests on the wave transmission over breakwaters with different porosities and permeabilityies performed. Nevertheless, differences in surface and volume porosity relative to each other together with the permeability of the core have not been investigated yet. So it is still unknown whether these differences in wave transmission are caused at the surface of the structure, or if this is caused at the core of the structure.

3

PHYSICAL MODEL

With the use of a physical model the influence of the permeability and porosity of artificial reefs on the wave transmission and velocities inside the structure is investigated. In this section, the scaling of the model, experimental setup in the flume and the performed runs are discussed.

3.1. SCALING

The empirical relations from section 2.2 are all results of physical models. Physical models are used to predict physical phenomena from reality in a down-scaled environment. A well-designed model should show similar behaviour to the prototype in real life. Physical modelling bridges the gap between what can be simulated accurately using numerical models and the real world (Kirkegaard et al., 2011).

However, considerable differences between the down-scaled model and the real-world prototype may result due to model, scale and measurement effects:

- *Model effects* result from incorrect reproduction of the prototype features such as geometry, fluid properties, and flow or wave generation techniques (Heller, 2011).

- *Scale effects* are a result of the inability to keep each force ratio constant between the real-world prototype and the model. Generally, scale effects increase with the scale factor (S. A. Hughes, 1993). The *scale factor* is the ratio between the characteristic length of the prototype and the model:

$$\lambda = \frac{L_p}{L_M} \tag{3.1}$$

Here L_p is the characteristic length in the real-world prototype (P) and L_m is the characteristic length in the model world (M), (Heller, 2011).

- *Measurement effects* are the non-identical measurement techniques used for data sampling in the model and prototype (Heller, 2011).

19

To get reliable results, the physical models have to fulfil geometrical, kinematical and dynamical similarity. With 'similarity', similar response of the model and prototype is meant. Similitude criteria are mathematical conditions that must be met by the scale ratios between the prototype and the real world. These criteria can be determined from mathematical representations of the physical properties (Yalin, 1971). Similarity can also be achieved if the similarity conditions are not met (S. A. Hughes, 1993).

3.1.1. SCALE RATIO'S

For a true similar physical model, for some phenomena in hydraulic engineering, the Froude number, Reynolds number and Weber number must be the same in the model and prototype (respectively represented in Equation 3.2, 3.3 and 3.4). However, this is not physically possible, unless $\lambda = 1$. In a Froude model, the wave field is dominated by the influences of gravity and inertia. If it can be ensured that the Reynolds number is sufficiently large to guarantee a fully turbulent flow, the Reynolds number can be neglected. The Weber number can also be neglected in situations where surface tension is negligible in prototype waves. However, it must be noted that this is only permitted if the wavelength is larger than 2 cm and the wave periods are longer than 0.35 seconds in the model (Kirkegaard et al., 2011).

$$Fr = \frac{u}{\sqrt{g \cdot L}} \tag{3.2}$$

$$Re = \frac{u \cdot L}{v_k} \tag{3.3}$$

$$We = \frac{\rho_w \cdot u^2 \cdot L}{\sigma} \tag{3.4}$$

Where:

u	[m/s]	=	flow velocity
L	[m]	=	length
g	[m/s^2]	=	gravitational acceleration
v_k	[m^2/s]	=	kinematic viscosity
ρ_w	[kg/m^3]	=	water density
H_s	[m]	=	significant wave height
D_n	[m]	=	armour rock diameter
σ	[kg^2]	=	surface tension

For this physical model, the Scheldt Flume of Deltares is used. As gravitational forces are dominant here, Froude scaling can be applied. Froude law can be used to scale down the forces. The Froude number should be the same in the model and prototype to yield a similar model. Equation 3.2 will be rearranged to the following scale ratio:

$$(\frac{u}{\sqrt{g \cdot L}})_p = (\frac{u}{\sqrt{g \cdot L}})_m \tag{3.5}$$

$$\frac{u_p}{u_m} = \sqrt{\frac{g_p}{g_m}\frac{L_p}{L_m}} \tag{3.6}$$

$$n_{Fr} = 1 = \frac{n_u}{\sqrt{n_g n_L}} \tag{3.7}$$

According to the Froude law, the scaling relations are expressed in terms of the length scale factors n_L:

Wave height (m)	n_H	=	n_L
Time (s)	n_T	=	$n_L^{0.5}$
Velocity (m/s)	n_u	=	$n_L^{0.5}$
Acceleration (m/s^2)	n_a	=	1
Mass (kg)	n_M	=	$n_\rho \cdot n_L^3$
Pressure (kN/m^2)	n_p	=	$n_\rho \cdot n_L$
Force (kN)	n_F	=	$n_\rho \cdot n_L^3$
Discharge (l/s/m)	n_q	=	$n_L^{1.5}$

In this model, a scale ratio of 20 is applied, based on the dimensions and limitation of the flume and the tested storm conditions. This means that a wave height of 0.25 m in the model, corresponds to a 5 m wave height in real-life. Note that the scale ratio is hypothetical, since there is no real structure being modelled. The scale serves as an indication. The analysis of the test will be based on Froude scaling such that the results should be valid for other scales as well.

3.2. EXPERIMENTAL SETUP
In accordance to Froude scaling, the experimental setup is designed. This includes the designs of the submerged breakwaters, flume setup, and input variables of the tests.

3.2.1. MODEL DESIGNS
To test the effect of *permeability* and *porosity* on the wave transmission and particle velocities inside the structure, five distinct breakwaters are tested in the Scheldt Flume at Deltares. A schematic representation of the designs can be found in Figure 3.1. More detailed information of Breakwater B, C, D, and E can be found in Appendix B.

Breakwater A Is an impermeable breakwater that is built with the dimensions that are presented in Figure 3.2. To ensure sufficient stability during the experiment, one vertical plate is placed over the cross-section at a distance of 0.5 m from the side.

Breakwater B Is a permeable breakwater consisting of rubble mound rocks. Epoxy is used to ensure stability of the stones during the test. This stability provides a constant permeability as no shifting of stones can occur. A diameter of 4 cm for the rocks is chosen. After construction of the breakwater, the exact porosity is determined by the weight and the volume of the structure. The exact porosity is 0.44, the calculation of this porosity and the construction can be found in Appendix B.

Breakwater C   Is a hollow perforated trapezoidal breakwater. Here, the surface poros-
ity of the perforated breakwater is the same as the volume porosity from structure B
($n \approx 0.44$). Furthermore, three velocity meters are placed 5 cm above the bed inside the
structure to measure the particle velocities.

Breakwater D   Is a hollow perforated trapezoidal breakwater with a vertical imperme-
able screen through the middle of the cross-section. It has a surface porosity of approxi-
mately 0.44. Two velocity meters are placed 5 cm above the bed to measure the streaming
velocities.

Breakwater E   Is a hollow perforated trapezoidal breakwater with a vertical perforated
plate in the middle. The perforated plate has the same surface porosity as the diago-
nal plates ($n \approx 0.44$). Moreover, two velocity meters are placed 5 cm above the bed to
measure the streaming velocities.

(a) Breakwater A   (b) Breakwater B   (c) Breakwater C

(d) Breakwater D   (e) Breakwater E
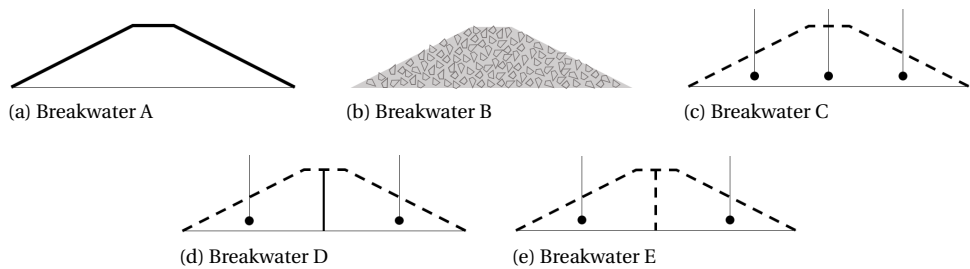
Figure 3.1: (a) impermeable breakwater, (b) rubble mound rock breakwater, volume porosity $n = 0.44$, (c) per-
forated hollow breakwater, surface porosity $n \approx 0.44$, (d) perforated hollow breakwater with a surface porosity
$n \approx 0.44$ and a vertical impermeable plate, (e) perforated hollow breakwater with a vertical perforated plate,
both with a surface porosity $n \approx 0.44$
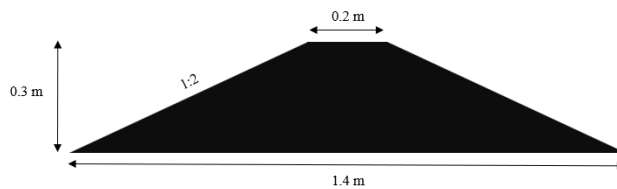
Figure 3.2: Model dimensions of a submerged breakwater

3.2.2. FLUME SETUP

The experiments were carried out in the Scheldt Flume at Deltares. This flume is 55 m long, 1 m wide and has a height of 1.2 m. Furthermore, it is equipped with an Active Reflective Compensation (ARC) in order to minimize the effect of reflecting waves in the flume. The maximum significant wave height that it can produce is 0.25 m ("Scheldt Flume - Deltares", n.d.).

A water depth of 0.75 m is chosen at the wave board since this is three times the maximum wave height. The length before the start of the transition slope is 26.55 m. This is longer than the required minimum of at least 3-5 times the water depth. This is for practical reasons as now, the breakwater is fully visible behind the glass of the flume. The structure is heightened to 0.35 m with a transition slope of 1:10 to reach the relative water depth, as shown in Figure 3.3.

The gauges are placed at a distance of 2 m, 2.44 m and 3 m from the structure. The distance between the three wave height meters are calculated by the program DISTANCEMF from Deltares. The horizontal part of the foreshore should be about two wave lengths before the first wave gauges. This is the distance that is needed to adjust to the new water depth. At the end of the flume, a wave absorber is placed to absorb all the wave energy to minimize reflection. Furthermore, in structure C, D and E, electromagnetic liquid velocity meters (EMS) are placed inside the breakwater to measure the water velocity. An overview of the flume setup is presented in Figure 3.3. In Figure 3.4, an overview of the instruments measuring the wave heights and velocities is visualised. In Appendix C, a more detailed description of the instruments used can be found.
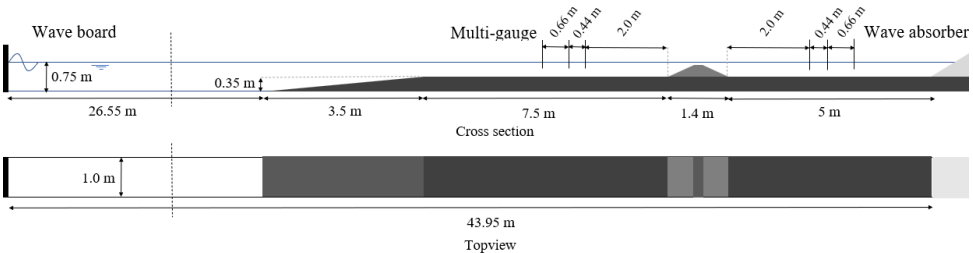
Figure 3.3: Overview of the flume setup
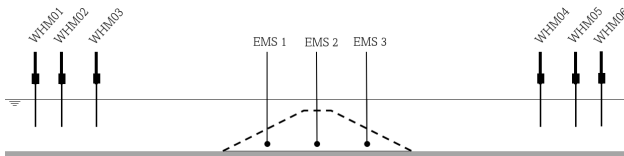
Figure 3.4: Sketch of the WHM and EMS in the wave flume

3.2.3. Test Conditions

The designs from Figure 3.1 are tested in the flume of Deltares for a duration of 1000 waves to obtain enough reliable data on the wave transmission. In Figure 3.5 an overview of the most important parameters in the experiment setup is presented. This is summarized in Equation 3.8.

$$K_t = \frac{H_t}{H_i} = f[h, R_c, d, T_p, \rho_w, H_i, H_t, B_c, v_k, g, n_{surface}, n_{volume}] \tag{3.8}$$

As the crest width and water characteristics are constant in all five experiments, some variables can be eliminated. Afterwords, the following variables influencing the wave transmission are left remain:

$$K_t = \frac{H_t}{H_i} = f[R_c, h, d, T_p, H_i, H_t, n_{surface}, n_{volume}] \tag{3.9}$$
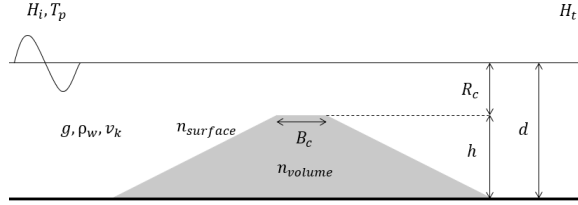
Figure 3.5: Definition of the governing parameters in the experiment setup

The most important variables that can be adjusted during the experiments are: wave steepness ($s_{m-1,0}$), water depth (d), significant wave height (H_{m0}) and peak period (T_p). Note that the wave steepness depends on the wave height and the wave period and is therefore not an independent variable. The permeability and porosity are varied by the different breakwater designs. Per breakwater, two wave steepnesses, four water depths and four wave heights are tested. For structure C and E two more water depths are tested, with three different wave heights. In total 208 tests were performed.

With Equation 3.10, the wave period resulting from the inserted wave height and wave steepness is calculated. In deep water, a Rayleigh distribution can be assumed. Here, a fixed ratio between the spectral period and sea-state period is valid. The ratio of the peak period (T_p) and the mean energy period ($T_{m-1,0}$) for a JONSWAP spectrum is assumed to be 1.107 (CIRIA et al., 2012). For the ratio between the mean period ($T_{m-1,0}$) and the mean energy period (T_m), 0.92 is found (Gerrit & Verhagen, 2016). An overview of the input variables is presented in Table A.1.

$$T_{m-1,0} = \sqrt{\frac{2\pi \cdot H_{m0}}{g \cdot s_{m-1,0}}} \tag{3.10}$$

Test ID	Parameter	Test input	Structure
$SXXX$	$S_{m-1,0}$	0.02, 0.04	A, B, C, D, E
$XdXX$	$d[m]$	0.25, 0.30, 0.35, 0.40, 0.45, 0.50	C, E
		0.35, 0.40, 0.45, 0.50	A, B, D
XXR_cX	$R_c[m]$	0.05, 0, -0.05, -0.10, -0.15, -0.20	C, E
		-0.05, -0.10, -0.15, -0.20	A, B, D
$XXXH$	$H_{m0}[m]$	0.10, 0.15, 0.20	C, E
		0.10, 0.15, 0.20, 0.25	A, B, D

Table 3.1: Experiment Input

The numbers of the Test ID have the following meaning;

- S: $[1,2] = [0.02, 0.04]$

- d: $[4,5,0,1,2,3] = [0.25, 0.30, 0.35, 0.40, 0.45, 0.50]$

- H: $[1,2,3,4] = [0.10, 0.15, 0.20, 0.25]$

- R_c: $[4,5,0,1,2,3] = [0.05, 0, -0.05, -0.10, -0.15, -0.20]$

For example, Test ID A1233 means; Breakwater A is tested with a wave steepness of 0.02, water depth of 0.45 m, wave height of 0.20 m and a crest freeboard of -0.20 m. For an overview of all input variables see Appendix A.

4

DATA ANALYSIS

This chapter discusses the analysis performed on the data collected during the experiments. First, the results from the measured wave transmission are analysed. Then, the orbital velocities measured inside Breakwater C, D, and E are elaborated upon.

Considerations that should be kept in mind when reading this chapter:

- The relative crest freeboard (R_c) is negative for submerged conditions.

- For the data analysis only submerged conditions ($R_c < 0$) are considered. The emerged conditions for Breakwater E and C are not analysed, but presented in Figure 4.2 for completeness.

- $T_{m-1,0}$ is used when analysing the results of the physical model as recommended by van Gent (1999). When the expected wave transmission is calculated from literature, the wave period stated in the literature (T_p or $T_{m-1,0}$) is used.

4.1. WAVE TRANSMISSION

This section is divided into four parts. First, the results from the physical model are discussed. Subsequently, the expected results considering the existing empirical relations from the literature review are analysed. The expected and measured results are then compared relative to each other. A new empirical relation for breakwaters A, B, and D is derived from these results. Lastly, the influence of the breakwaters on the wave spectra is analysed.

4.1.1. RESULTS FROM THE PHYSICAL MODEL

To facilitate the interpretation of the data, the designs discussed in chapter 3 are presented again in Figure 4.1.

| (a) Breakwater A | (b) Breakwater B | (c) Breakwater C | (d) Breakwater D | (e) Breakwater E |
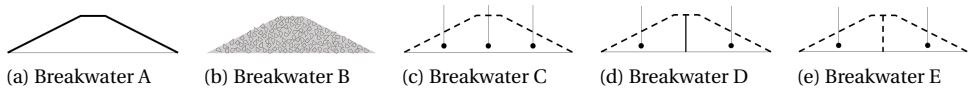
Figure 4.1: Design of the breakwaters that were tested in the physical model

Following from the measured water levels by the wave height meters, the wave heights are calculated using the Mansard and Funke method. With this method, the reflections from the wave absorber and breakwater are excluded from the measured water levels which results in the incoming and transmitted wave height. These wave heights are used when calculating the wave transmissions.

In total, 208 tests were performed which resulted in the wave transmissions that are presented in Table 6.1 and Figure 4.4. From this, it can be concluded that Breakwater C and E, and Breakwater A, B, and D showed similar wave transmissions. The wave transmissions for Breakwater C and E are too high to function as a coastal breakwater. Breakwater E and C have in common that they both are hollow perforated breakwaters where Breakwater E has an additional perforated vertical plate in the cross-section. From this, it can already be concluded that the core of a perforated submerged breakwater greatly influences the wave transmission.

	A	**B**	**C**	**D**	**E**
K_t	0.54-0.96	0.62-0.92	0.82-0.95	0.57-0.89	0.77-0.93

Table 4.1: Measured wave transmissions
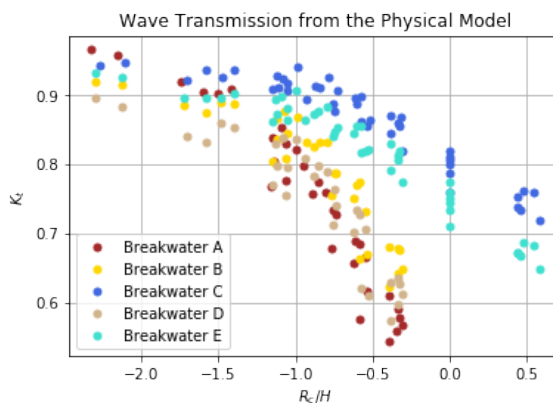
Figure 4.2: Measured wave transmission from Breakwater A, B, C, D, and E

Furthermore, according to van der Meer et al. (2005), the smooth impermeable break-water (A) should result in higher wave transmissions than the rubble mound breakwater (B) as no energy dissipation at the crest can occur due to the absence of the hydraulic roughness and permeability at the armour layer.

The results of this experiment show that the permeable rubble mound breakwater (B) results in higher wave transmissions, and therefore it could be concluded that the hydraulic roughness and permeability of the armour layer do not result in significant extra wave dissipation. The permeability of the core at Breakwater B could explain the increase in wave transmission compared to Breakwater A.

In the following sections, the effects of the dimensionless parameters, relative crest freeboard (R_c/H), wave steepness (H/L), relative crest width (B_c/L), and relative structure height (h/H), will be further analysed.

4.1.2. INFLUENCE R_c/H_s

In Figure 4.4 the breakwaters are compared to each other. Hereby, an exponential regression is applied to expose differences in dependency. For the exponential regression analysis the following formula is applied:

$$K_t = a \cdot e^{R_c/H_s} + b \tag{4.1}$$

With using exponential regression, the values a and b for each breakwater are calculated and presented in Table 4.2. In Figure 4.3 the dependency of the wave transmission on R_c/H_s is visualised.

	A	B	C	D	E
a	-0.67	-0.46	-0.14	-0.48	-0.17
b	1.04	0.99	0.96	0.96	0.93

Table 4.2: Exponential regression of the wave transmission relative to R_c/H_s for Breakwater A, B, C, D, and E
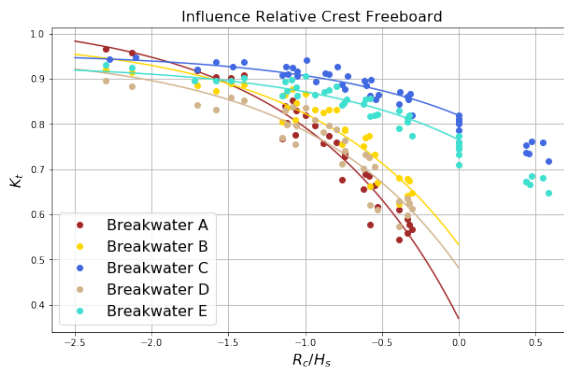
Figure 4.3: Influence of the relative crest freeboard on the wave transmission for breakwater A, B, C, D, and E

In Figure 4.4 the different breakwaters are compared to each other.

- From Figure 4.4 a) and Table 4.2, it can be concluded that Breakwater D and E show different behaviours with respect to the relative crest freeboard. As Breakwater E shows little wave dissipation, it can be concluded that the vertical impermeable plate, as applied for Breakwater D, is causing most of the decrease in wave transmission.

  Thereby, Breakwater D and E look similar from the outside, however they result in very different wave transmissions. This is valuable information for the design of artificial reefs, as both designs enhance a sheltered habitat for marine life. However, by adding an impermeable plate, the primary function of coastal protection, by dissipating wave energy, is also achieved with Breakwater D.

- From Figure 4.4 b) and Table 4.2, it is observed that Breakwater A and D show similar wave transmissions. However, Breakwaters A and D do not show the same dependency on R_c/H_s, meaning that the shape of the impermeable layers or the perforated outer layer of D is causing a different dependency on the relative crest freeboard. van der Meer and Daemen (1994) hypothesised that the shape of submerged breakwaters is not significant for the wave transmission. However, as can be seen from Figure 4.4 b), as R_c/H approaches 0, the wave transmission of Breakwater A is higher than Breakwater D. This could be explained by the suggestion that when R_c approaches 0, the shape of the impermeable structure does influence the wave transmission.

- From Figure 4.4 c) and Table 4.2, it is observed that Breakwater B and D show a similar dependency on the relative crest freeboard. Placing a vertical impermeable screen in a hollow perforated breakwater, as done in Breakwater D, causes the surface porosity to determine the dependency on the relative crest freeboard. Furthermore, they show similar wave transmissions. However, Breakwater B shows a consistently 0.3 higher wave transmission than Breakwater D. From this it can be hypothesized that the hydraulic roughness and friction in the structure of Breakwater B is not adding significant wave dissipation.

- From Figure 4.4 d) and Table 4.2, it is observed that Breakwater B and C show different dependencies on R_c/H_s and thereby differ greatly in wave transmission. From this, it can be concluded that the wave transmission is greatly affected by the volume porosity, if the friction inside the structure is assumed to be negligible.

- From Figure 4.4 e) and Table 4.2, it is observed that Breakwater C and E show similar dependency on R_c/H_s, although less dependency on R_c/H_s than other breakwaters. Moreover, Breakwater C shows a consistently 0.3 higher wave transmission than Breakwater E. The perforated plate in the cross-section results in extra blocking of the orbital motion inside the breakwater, which results in this small decrease in wave transmission.

- From Figure 4.4 f) and Table 4.2, it is observed that Breakwater A and B show a different dependency on the relative crest freeboard. The wave transmissions show similar results. From this, it can be concluded that the porosity of Breakwater B has little influence on the wave transmission compared to Breakwater A.
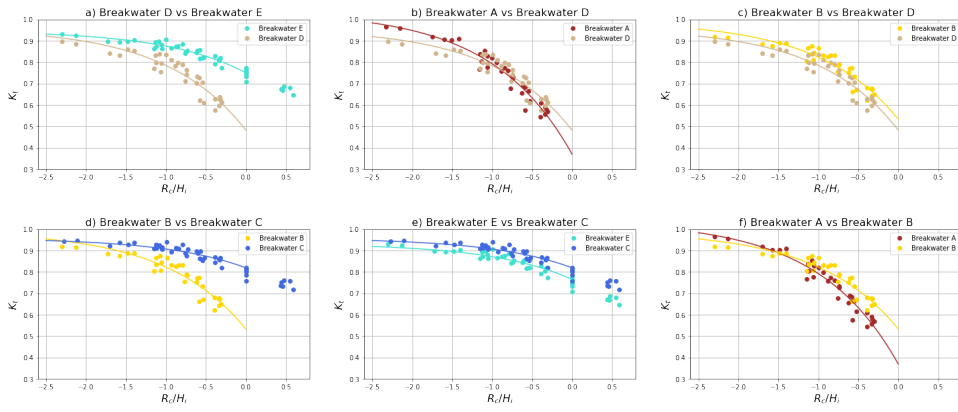
Figure 4.4: Comparison between the different breakwaters relative to R_c/H_s

4.1.3. INFLUENCE H_s/L

In Figure 4.5 the wave transmission relative to the wave steepness is presented. Linear regression is used to identify any characteristic behaviour of the breakwaters.

$$K_t = a \cdot H_s/L + b \tag{4.2}$$

The variables of a and b resulting from the linear regression analysis are presented in Table 4.3. In Figure 4.5 the influence of H_s/L on the wave transmission is presented for the different breakwaters.

d [m]	A				B				C				D				E			
	0.35	0.40	0.45	0.50	0.35	0.40	0.45	0.50	0.35	0.40	0.45	0.55	0.35	0.40	0.45	0.50	0.35	0.40	0.45	0.50
a	-3.83	-7.01	-9.02	-7.54	-2.03	-3.11	-3.12	-2.89	0.15	-0.82	-1.00	-1.06	-1.60	-2.96	-2.80	-3.00	-0.68	-0.92	-1.27	-1.76
b	0.72	0.96	1.13	1.14	0.73	0.89	0.95	0.98	0.85	0.99	0.95	0.97	0.67	0.84	0.90	0.96	0.83	0.88	0.92	0.96

Table 4.3: Linear regression of the wave transmission relative to H_s/L for Breakwater A, B, C, D, and E
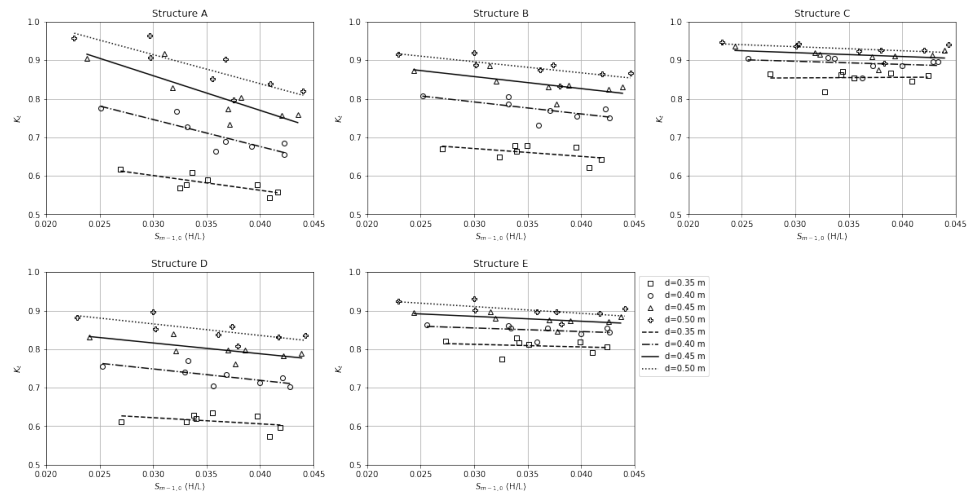
Figure 4.5: Influence of the wave steepness on the wave transmission for Breakwater A, B, C, D, and E

From Figure 4.5 and Table 4.3 it can be concluded that there is little influence of the wave steepness (H_s/L) on the wave transmission. The numbers in Table 4.3 could be misleading as the values of a are high, but the range of the wave steepness is small (from 0.01 to 0.05) and therefore results in small differences in wave transmission.

For Breakwater C and E the influence is almost 0. For Breakwater B and D there is a small influence of the wave steepness. It can be observed that for Breakwater A the influence of H_s/L increases with the water depth. The steeper waves are hypothesized to dissipate more energy as they feel the structure more than the waves with a low wave steepness that have the chance to move over the breakwater without feeling the structure and therefore not dissipate energy. At Breakwater B and D, for low wave steepness's dissipation could be caused by the surface porosity which explains the lower dependency on the wave steepness in deeper water.

In general, shorter waves (higher $s_{m-1,0}$ value) result in lower wave transmissions. For Breakwater A there is a significant influence of H_s/L when the water depth increases. However, because here the wave transmissions are high, it is irrelevant for the design of breakwaters as a breakwater will not be designed for such high wave transmissions. Therefore, the influence of H_s/L in practice will be marginal.

4.1.4. Influence B_c/L

In Figure 4.6 the wave transmission is presented relative to the relative crest width (B_c/L). Here again, linear regression is used to identify characteristic behaviour of the breakwaters. The variables of a and b resulting from linear regression are presented in Table 4.4. In Figure 4.6 the wave transmissions relative to B_c/L are visualised.

$$K_t = a \cdot B_c/L + b \tag{4.3}$$

	A				B				C				D				E			
d [m]	0.35	0.40	0.45	0.50	0.35	0.40	0.45	0.50	0.35	0.40	0.45	0.55	0.35	0.40	0.45	0.50	0.35	0.40	0.45	0.50
a	-0.37	2.28	4.61	4.33	-0.36	1.30	2.13	2.01	0.58	0.95	0.72	0.87	-0.47	1.23	1.82	2.25	0.46	0.63	0.95	1.38
b	0.60	0.59	0.58	0.67	0.68	0.70	0.73	0.79	0.82	0.84	0.88	0.89	0.64	0.67	0.71	0.74	0.78	0.82	0.83	0.84

Table 4.4: Linear regression of the wave transmission relative to B_c/L for Breakwater A, B, C, D, and E
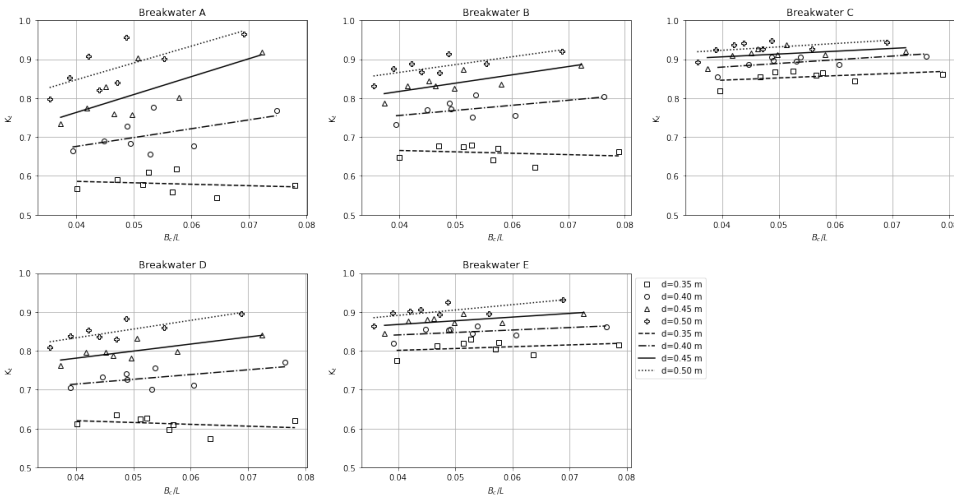
Figure 4.6: Influence of the relative crest width for Breakwater A, B, C, D and E

As the crest width (B_c) is kept constant during the experiments, the range of B_c/L is relatively small. Here, a range of 0.035-0.08 for B_c/L is tested to submerged structures with a relatively narrow crest. However, characteristic behaviour of the breakwaters relative to B_c/L could still be observed.

From Figure 4.6 and Table 4.4 it is observed that Breakwater C and E show little to no dependency to B_c/L. Breakwater B and D show similar dependencies as well. For Breakwater A, the biggest dependency on B_c/L is observed when the water depth increases. This is remarkable, as van der Meer et al. (2005) suggest that B_c/L would be of negligible influence for smooth impermeable breakwaters. But here, it is the structure with the most influence on B_c/L. If the hydraulic roughness of rubble mound breakwaters indeed would result in extra wave dissipation, a stronger influence of B_c/L for Breakwater B would be expected, which is not the case. This again indicates that the influence of the hydraulic roughness and friction has no significant influence for submerged breakwaters.

4.1.5. Influence h/H_s

In Figure 4.7 the wave transmissions relative to h/H_s are presented. Linear regression is applied here too. The following formula is applied:

$$K_t = a \cdot h/H_s + b \tag{4.4}$$

d [m]	A				B				C				D				E			
	0.35	0.40	0.45	0.50	0.35	0.40	0.45	0.50	0.35	0.40	0.45	0.55	0.35	0.40	0.45	0.50	0.35	0.40	0.45	0.50
a	0.014	0.060	0.090	0.076	0.0042	0.032	0.038	0.033	0.010	0.016	0.014	0.014	0.00	0.030	0.033	0.035	0.012	0.013	0.016	0.022
b	0.55	0.57	0.61	0.72	0.65	0.70	0.76	0.81	0.83	0.86	0.88	0.90	0.61	0.66	0.73	0.77	0.78	0.82	0.84	0.85

Table 4.5: Linear regression of the wave transmission relative to h/H_s for Breakwater A, B, C, D, and E
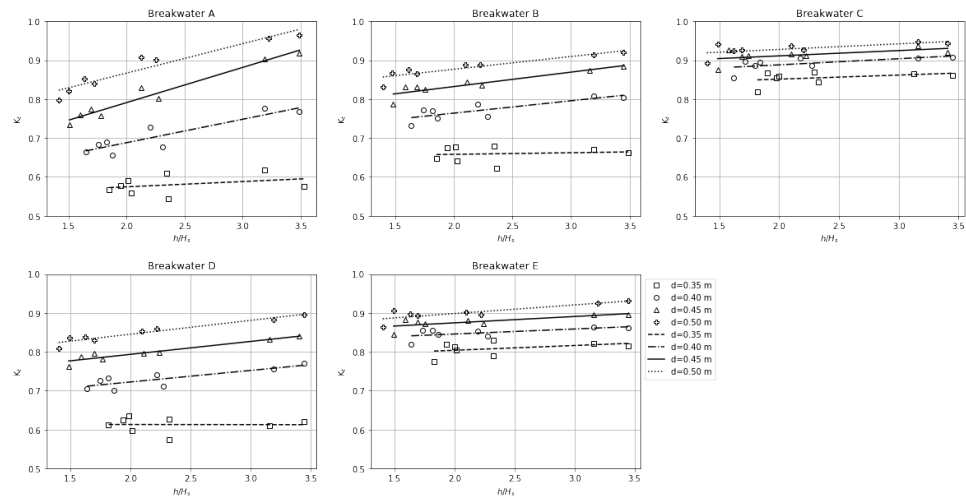
Figure 4.7: Influence of h/H_s on the wave transmission for breakwater A, B, C, D, and E

From Figure 4.7 and Table 4.5 it can be concluded that Breakwater C and E again show little dependency on h/H_s. Breakwater B and D show similar behaviour and Breakwater A shows the most dependency on h/H_s. Moreover, for Breakwater A, the influence

of h/H_s increases when the water depth increases. Apparently, at low water depths all waves feel the structure. But when it gets deeper, some waves will feel the structure and others will not. For Breakwater B and D, the surface porosity will always cause some energy dissipation, also for the longer waves.

4.1.6. CONCLUSION OF RELEVANT PARAMETERS AND BREAKWATERS OF INTEREST

Concluding from the physical model results, the parameter affecting the wave transmission the most is the relative crest freeboard (R_c/H). B_c/L, H_s/L, and h/H_s showed little dependency on the wave transmission. For these three parameters, when the water depth increased the dependency on the parameter for Breakwater A, increased as well. This is likely because at lower water depths all waves feel the structure, but when it gets deeper, and the water depth above the structure increases, some waves feel the structure and others do not. This becomes mostly visible at the higher wave transmission in deeper water. However, no breakwater will be built for these high wave transmissions, therefore they do not significant impact the wave transmissions.

The theory by van der Meer et al. (2005) that the hydraulic roughness and permeability of the armour layer result in extra wave dissipation is neither confirmed nor rejected by the results of this physical model. But the statement that a permeable low-crested structure in general results in less wave transmission than the same impermeable structure, is rejected.

The breakwaters that are considered to be of most interest resulting from the physical model are Breakwater A, B, and D. This is because they show similar wave transmissions but differ greatly in design which could be of use for the design of artificial reefs.

4.1.7. EXPECTED RESULTS FROM THE EXISTING EMPIRICAL RELATIONS

From the literature review in chapter 2, the empirical formulations of van der Meer (1990), d'Angremond et al. (1996), Bleck and Oumeraci (2001), Friebel and Harris (2003), and van der Meer et al. (2005) are used to predict the wave transmissions.

Using the input variables from the physical model which are listed in Appendix A, and the empirical formulations from Table 2.2, the expected wave transmissions are calculated and presented in Figure 4.8. Notice that the expected results from Bleck and Oumeraci (2001) are not presented in this figure as there is no dependency on R_c/H_s in this formula.
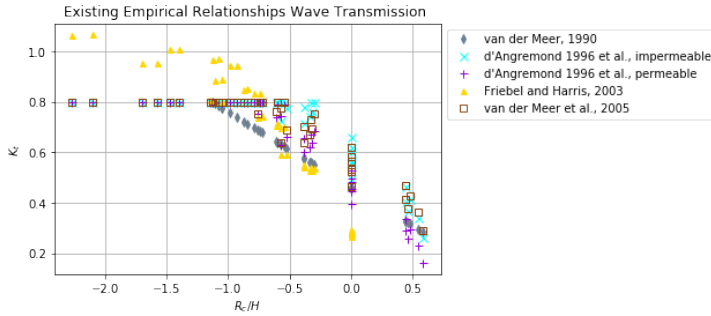
Figure 4.8: Wave transmission according to van der Meer (1990), d'Angremond et al. (1996), Friebel and Harris (2003), and van der Meer et al. (2005)

From Figure 4.8 it can be concluded that according to van der Meer (1990) and d'Angremond et al. (1996) the wave transmission will never exceed 0.8. Moreover, according to d'Angremond et al. (1996), the wave transmission for permeable breakwaters is lower than for impermeable breakwaters. The best empirical fit from Friebel and Harris (2003) does allow wave transmissions above 0.8, even some wave transmissions that slightly exceed 1.0. This is not physically impossible, but only happens rarely.

4.1.8. RESULTS COMPARED TO LITERATURE

Subsequently, the results of the physical model are compared to the existing empirical relationships. In Figure 4.9 an overview of the results from the physical model and literature is presented.
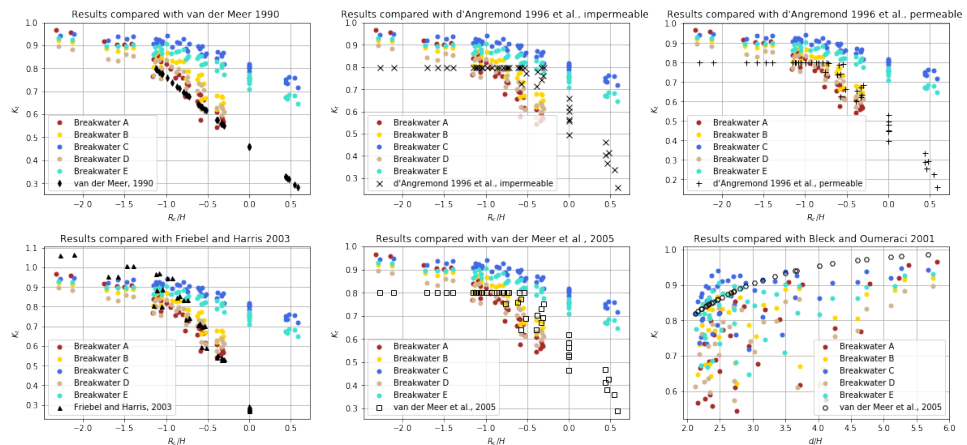
Figure 4.9: Comparison between the existing empirical relationships and measured wave transmissions

To quantify the applicability of the existing empirical relations, the Root Mean Squared Error (RMSE) is calculated and presented in Table 4.6, with N the number of experiments performed per breakwater.

$$RMSE = \sqrt{\frac{\Sigma(K_{t,predicted} - K_{t,measured})^2}{N}} \tag{4.5}$$

	A	B	C	D	E
van der Meer, 1990	**0.042**	0.095	0.23	0.060	0.18
d'Angremond et al., 1996, impermeable	0.12	0.074	0.11	0.090	0.076
d'Angremond et al., 1996, permeable	0.079	**0.052**	0.15	**0.044**	0.11
Bleck and Oumeraci, 2001	0.19	0.14	**0.044**	0.17	**0.059**
Friebel and Harris, 2003	0.074	0.086	0.18	0.092	0.15
van der Meer et al., 2005	0.093	0.056	0.13	0.059	0.097

Table 4.6: Overview of the RMSE from existing empirical relations

From Table 4.6 it can be concluded that for Breakwater A, the relation found by van der Meer (1990) is the best fit, for Breakwaters B and D d'Angremond et al. (1996) provides the best fit, and for Breakwaters C and E, Bleck and Oumeraci (2001) provides the best match. Friebel and Harris (2003) and van der Meer et al. (2005) are not the most accurate fit for any of the breakwaters.

4.1.9. DERIVING A NEW EMPIRICAL RELATIONSHIP FOR THE WAVE TRANSMISSION

From subsection 4.1.1 it was concluded that the most import parameter influencing the wave transmission is R_c/H_s. Moreover, Breakwater A, B, and D showed similar wave transmissions and Breakwater B and D show similar dependencies on the dimensionless parameters. Also, from the current literature, one design formula to predict the wave transmission for breakwaters like A, B, and D is lacking. Therefore , a new formula for predicting the wave transmission over submerged breakwaters is derived here.

As R_c/H_s was considered to be the most important parameter, initially only the exponential dependency on R_c/H_s is taken into account. With an exponential regression analysis, this resulted in the following formula:

$$K_t = -0.53 \cdot e^{\frac{R_c}{H_s}} + 1.0 \tag{4.6}$$
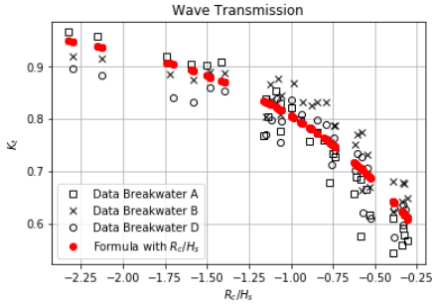
(a) Newly predicted wave transmissions using Equation 4.6
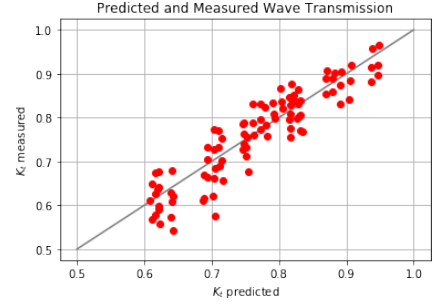
(b) Expected and measured wave transmissions using Equation 4.6 resulting in a RMSE of 0.041

Figure 4.10: Wave transmissions calculated using Equation 4.6

	A+B+D	A	B	D
RMSE	0.041	0.045	0.040	0.038

Table 4.7: Root mean squared error using Equation 4.6 for Breakwater A, B, and D

The RMSE's from Table 4.7 are no improvement on the existing literature presented in Table 4.6 as the RMSE is higher than in the existing empirical relations. Therefore another parameter should be taken into account to improve the formula and decrease the RMSE.

The other three dimensionless parameters that had similar influence on the wave transmission were B_c/L, H_s/L, and h/H_s. H_s/L does not contain a dimension parameter from the structure and therefore will not contribute to the design phase of artificial reefs. The next parameter to be taken into account is h/H_s, as here, the structure height is made dimensionless by the same parameter as the relative crest freeboard. From this, a multiple regression analysis is applied, resulting in the following formula:

$$K_t = -0.59 \cdot e^{\frac{R_c}{H_s}} - 0.042 \frac{h}{H_s} + 1.12 \tag{4.7}$$

With a range of validity of:

$$0.014 \leq \frac{H}{L} \leq 0.032$$

$$0.6 \leq \frac{h}{d} \leq 0.86$$

$$-2.30 \leq \frac{R_c}{H_s} \leq -0.3$$

$$1.2 \leq \frac{h}{H_s} \leq 3$$

It can be observed that after using Equation 4.7, the influence of the relative crest height has almost doubled, making the relative crest height still the most important parameter influencing the wave transmission. In Figure 4.11, Equation 4.7 is plotted and in Table 4.8 the RMSE's are presented. From this it can be concluded that Equation 4.7 is a slight improvement for Breakwater A, and a significant improvement for Breakwater B and D compared to existing empirical relations.
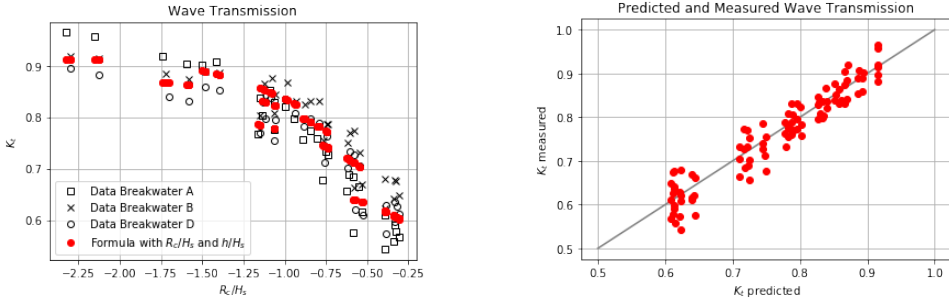
(a) New predicted wave transmissions using Equation 4.7

(b) Expected and measured wave transmissions using Equation 4.7 resulting in a RMSE of 0.032

Figure 4.11: Wave transmissions calculated using Equation 4.7

	A+B+D	A	B	D
RMSE	0.032	0.040	0.031	0.023

Table 4.8: Root mean squared error using equation Equation 4.7 for Breakwater A, B, and D

In Figure 4.12 the influence of the parameters R_c/H_s and h/H_s is visualised within the range of validity. From this, it can be seen that h/H_s has less influence on the wave transmission than R_c/H_s
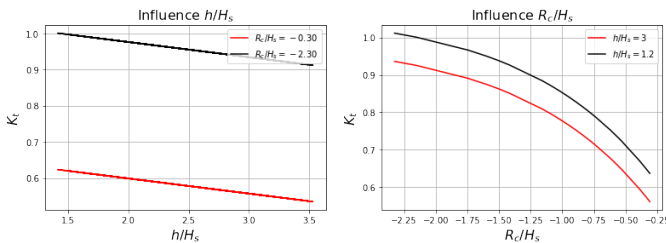
Figure 4.12: Visualisation of the influence of the parameters R_c/H_s and h/H_s

In Figure 4.13 an overview of the current empirical relation compared to Equation 4.7 for each breakwater is presented. From Figure 4.13 it is visible that the new formula

represents the measured wave transmissions better than the existing empirical relations by van der Meer (1990) and d'Angremond et al. (1996), permeable.
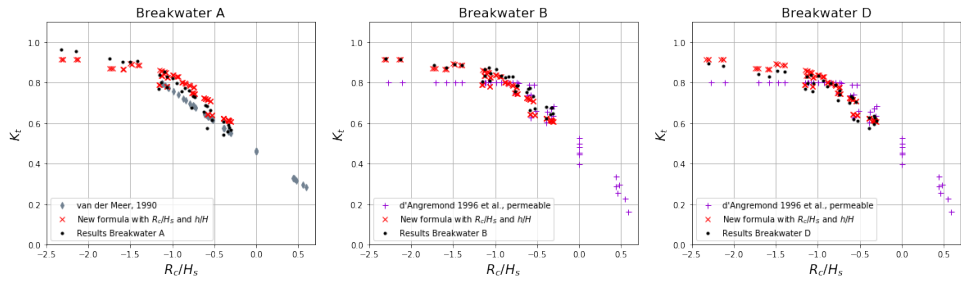
Figure 4.13: Overview of the existing empirical relations compared to the new formula for Breakwater A, B, and D

4.2. WAVE SPECTRUM

For the design of a breakwater it is valuable to know how the wave spectrum on the lee side of the breakwater is transmitted. For example, for a harbour, long waves could be disadvantageous as ships will experience more swell in the harbour that can lead to damage of the ships. Therefore, in this section the influence of the breakwater on the wave spectrum is investigated. This is done by analysing changes in T_p and $T_{m-1,0}$.

The peak period (T_p) is the wave period of the spectrum with the highest wave energy. The wave period ($T_{m-1,0}$) is the wave period that is based on the zeroth and first negative spectral moment. This wave period gives more weight to the energy at the lower frequencies. It was numerically concluded by van Gent (1999) that the spectral wave period $T_{m-1,0}$ is the optimal wave period for non uni-model spectra. This was confirmed by van Gent (2001) with physical model tests.

4.2.1. PEAK PERIOD

In Figure 4.14 the period ratio $T_{p,t}/T_{p,i}$ is presented in relation to the wave transmission, K_t. In Appendix D the wave spectra of the tests marked in Figure 4.14 are visualised.

From Figure 4.14 it can be concluded that the peak wave period is slightly increased, meaning that the most energetic waves are transferred to the lower frequencies. This is in line with the findings of van der Meer et al. (2000), who stated that the peak period may not increase more than 10% relative to the incoming wave spectrum. There is no significant difference between the different breakwaters.
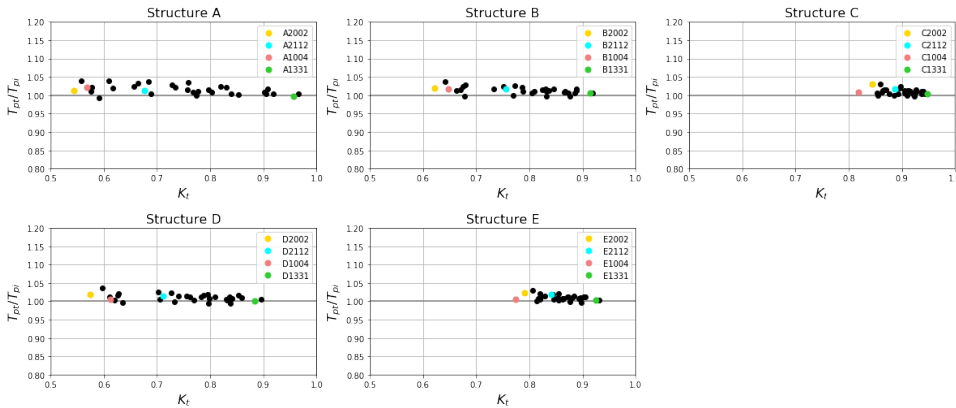
Figure 4.14: Change in peak wave period over Breakwater A, B, C, D, and E

4.2.2. MEAN PERIOD

From Figure 4.15 it can be concluded that for the smooth impermeable breakwater (A), $T_{m-1,0}$ is always decreased after the breakwater, indicating a shift to the lower frequencies in the wave spectrum. This is caused by the wave breaking which results in a reduction of the wave energy. For Breakwater B and D, $T_{m-1,0}$ is mostly decreased as well. Moreover, in general, the higher the wave transmission, the smaller the change in wave period.

For Breakwater C and E, the perforated permeable breakwaters, a less clear correlation with K_t can be observed. $T_{m-1,0}$ is mostly increased meaning that the energy of the wave spectrum is shifting more to the lower frequencies.

In conclusion, Breakwater C and E transmit mostly longer waves. For breakwater A, B, and D mostly shorter waves are transmitted over the breakwater.

According to van der Meer et al. (2000), if the reduction in wave energy is mainly caused by the flow *through* the armour layer, higher frequencies could be cut. In Figure 4.16 the wave spectrum changes of test 1004 are visualised. These wave spectra are based on the raw wave height data and calculated with the use of a Fourier transformation. The results show that for Breakwater A, B and D, the higher frequencies are cut. This indicates that for Breakwater C and E, the energy dissipation primary takes place at the surface of the breakwaters and not by friction *through* the structure. This makes sense as the breakwaters are almost fully hollow and permeable. For Breakwater B, the rubble mound breakwater, the cut in highter frequencies indeed could be explained by the flow *through* the structure. For Breakwater A and D however, this can not be valid. What these structures have in common is that they both have an impermeable screen. From this, it is concluded that not only the flow *through* the structure is causing a cut in the higher frequencies, as suggested by van der Meer et al. (2000), but the *permeability* of the screen as well.
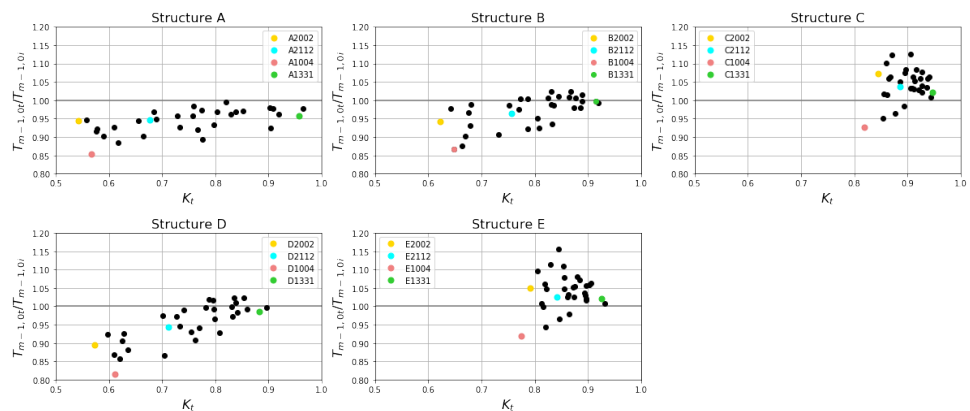
Figure 4.15: Change in mean spectral wave period over Breakwater A, B, C, D, and E
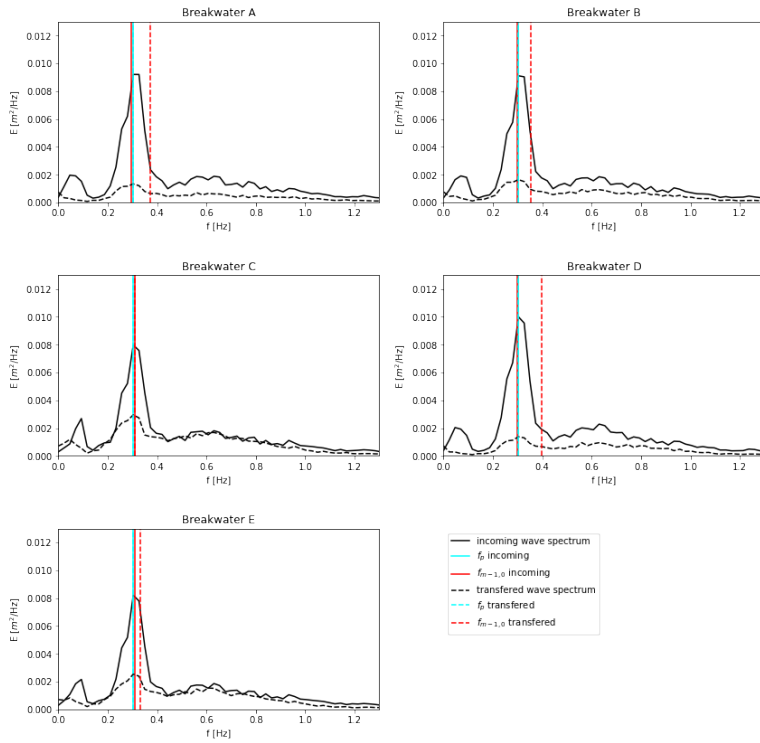
Figure 4.16: Wave spectrum changes test 1004, (S = 0.02, d = 0.35 m, R_c = 0.05 m, H = 0.25 m)

4.3. ORBITAL VELOCITIES

In this section, the orbital velocities measured in Breakwater C, D, and E will be discussed. The measured orbital velocities are used to draw conclusions about the effect of the breakwater on the velocity inside the structure. From this, the primary function of artificial reefs, which is creating a sheltered habitat for marine life, can be investigated.

Here, the focus lies on the orbital velocity induced by waves only. However, as artificial reefs are located at the foreshore, also other processes such as wind and tide will cause a current velocity. Yet in the physical model only the wave-induced orbital velocities for storm conditions are measured. These are the most critical velocities which could cause damage to artificial reefs.

First, the data from the physical model will be analysed. Subsequently, the orbital velocities are calculated that are expected when no breakwater is present. Finally, the results of the physical model will be compared to previously calculated velocities.

4.3.1. RESULTS FROM THE PHYSICAL MODEL

In Figure 4.17, 4.18, and 4.19 the horizontal orbital velocities from the physical model are presented relative to respectively the water depth (d), wave height (H), and wave length (L). Here, the focus lies on the maximum velocities in the onshore and offshore direction as they can cause dislodgement or deformation of the marine life that is located in the artificial reef. The mean of the orbital velocity is around 0 and therefore not important. $u_{onshore}$ and $u_{offshore}$ are calculated by taking the mean of the top and lower 10% of the data. Here again, the emerged conditions of Breakwater C and E are not taken into account.

From Figure 4.17 it is observed that Breakwater C, D, and E have a weak correlation with the water depth. In Figure 4.18 and 4.19 there is observed a correlation with the wave height and wave length for Breakwater D. Here, Breakwater C and E show a weak correlation again.

Moreover, it is observed that Breakwater C and E show similar velocities which is expected as from the wave transmission it already was concluded that the vertical perforated plate does not have much impact on the hydraulic performance of the breakwater. This also explains the similarity between the velocities measured by EMS 1 and EMS 3 for Breakwater C and E. Therefore, the analyses of the orbital velocities from now on will be solely focused on Breakwater D.

It can be observed that for $u_{onshore}$ at Breakwater D, EMS 3 shows a wider range of velocities whereas for $u_{offshore}$, EMS 1 shows a wider range of velocities. This is caused by the vertical impermeable plate which blocks the velocity and therefore limits the onshore and offshore velocity dependent on the direction of the waves.
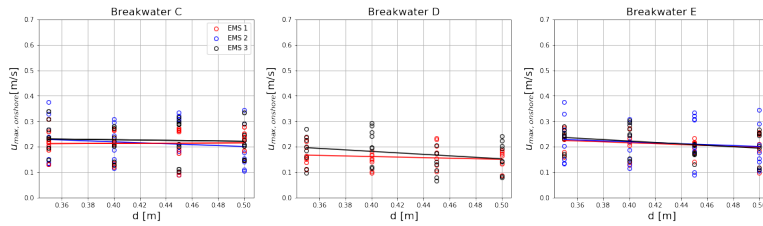
(a) $u_{x,onshore}$ relative to d
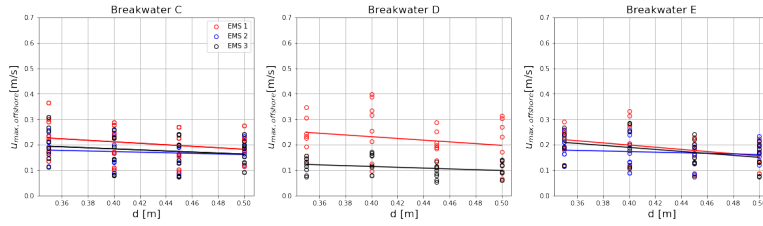
(b) $u_{x,offshore}$ relative to d

Figure 4.17: Maximum onshore and offshore velocity relative to the water depth (d)
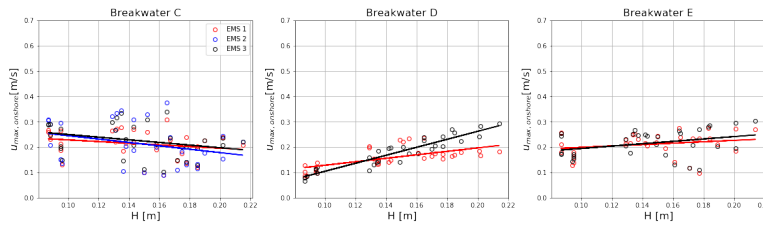
(a) $u_{x,onshore}$ relative to H
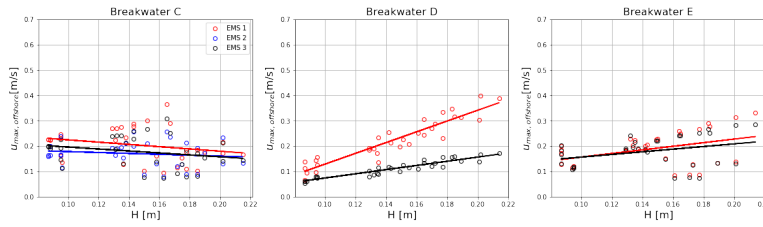
(b) $u_{x,offshore}$ relative to H

Figure 4.18: Maximum onshore and offshore velocity relative to the wave height (H)

(a) $u_{x,onshore}$ relative to L

(b) $u_{x,offshore}$ relative to L
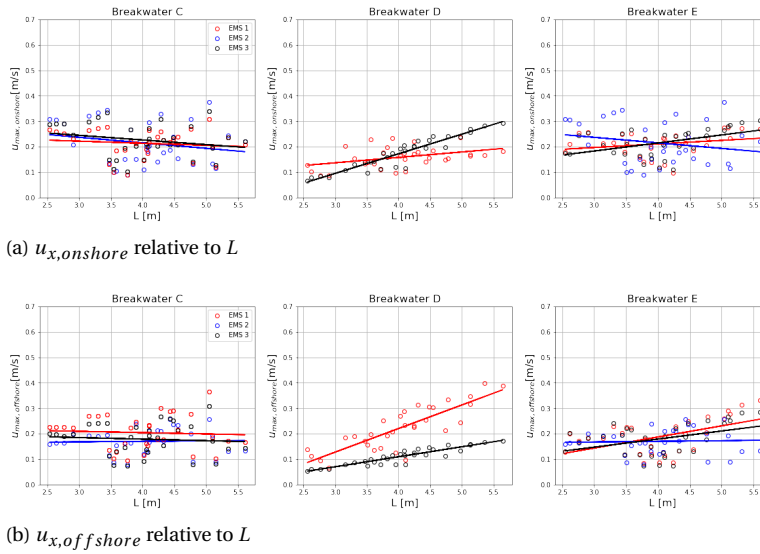
Figure 4.19: Maximum onshore and offshore velocity relative to the wave length (L)

4.3.2. MARINE LIFE

$u_{onshore}$ and $u_{offshore}$ are of interest for the dislodgement and movement limits of marine life as those limits might be exceeded during storms. This can cause damage to the artificial reef. For the feeding limits the velocity caused by other processes such as wind and tide will be of more importance as the mean of the orbital motion caused by waves lies around 0 and therefore will not contribute to reaching these feeding limits. Therefore, in this section the focus will be on the dislodgement, movement, and deflection limits of the species mentioned in section 2.1 Table 2.1.

To use these velocities in the physical model, the scaling factor of 20 is applied. The velocities from Table 2.1 are divided by $\sqrt{20}$ to achieve similarity to the downscaled model.

The velocities are presented in Figure 4.20 relative to L, including the limit velocities of the organisms from section 2.1.
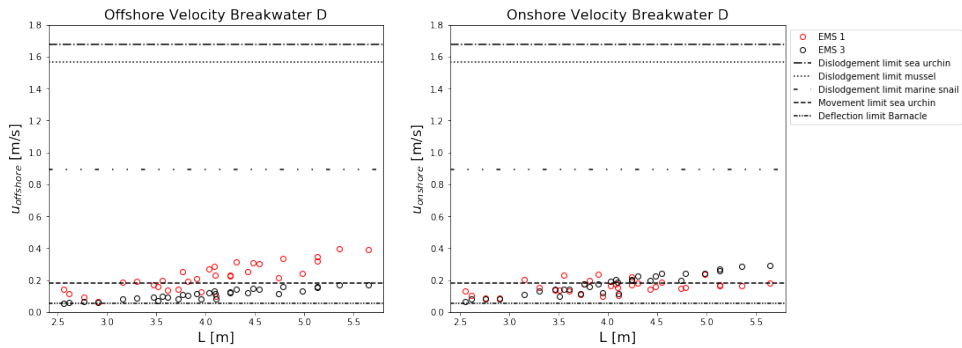
Figure 4.20: Onshore and offshore velocities relative to the wave length including the velocity limits of the marine life

From Figure 4.20 it can be concluded that the dislodgement velocities of the marine snail, sea urchin, and mussel are never exceeded and therefore these species will be able to find shelter in Breakwater D. For the barnacle the deflection limit is exceeded in all experiments. The movement limit of the sea urchin is exceeded for half of the tests at EMS 1, and for none at EMS 3.

From this, it can be concluded that Breakwater D could function as a sheltered habitat for almost all organisms presented in Table 2.1, and therefore could function as an artificial reef besides its secondary function as a coastal breakwater.

4.3.3. Calculated Orbital Velocity

In this section, the expected horizontal orbital velocity is calculated outside the structure. Because $kd<1$, a shallow water condition is assumed. Following from this, the depth-uniform velocity amplitude is given by Equation 4.8 (Holthuijsen, 2007).

$$\hat{u}_x = \frac{\omega a}{kd} \qquad (4.8)$$

Where:

ω = angular frequency ($2\pi/L$)
k = wave number ($2\pi/T$)
d = water depth
a = wave amplitude ($H/2$)

and:

$$L = T\sqrt{gd} \qquad (4.9)$$

For calculating the expected orbital velocities, the mean energy period ($T_{m-1,0}$) and significant wave height (H_s) of Breakwater C measured before the structure are used. This data is less influenced by the breakwater itself as little wave reflection and a high wave transmission was measured. Therefore, this data is the most similar to a situation without a breakwater.

The calculated velocities are presented in Figure 4.21. A correlation between u_x and L and H is observed. The correlation with the water depth (d) is weak.
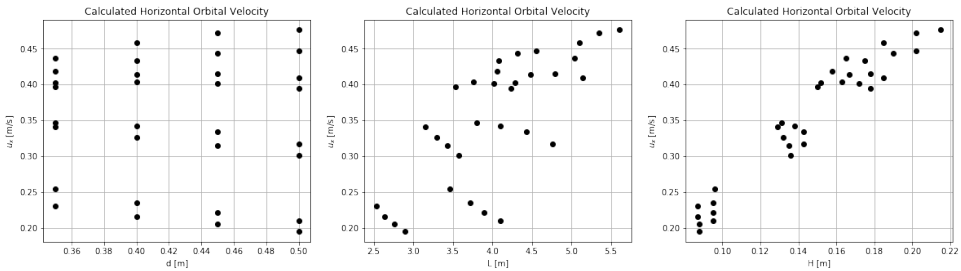
Figure 4.21: Calculated horizontal velocity relative to the water depth (d), wavelength (L), and wave height (H)

4.3.4. Measured Velocities Compared to Calculated Velocities

By using the calculated velocities, the influence of the breakwater on the orbital velocities close to the shore can be determined. In Figure 4.22 the calculated velocities from Equation 4.8 and the maximum onshore and offshore velocities from the physical model are compared relative to each other. Here, it is assumed that the calculated velocity is the same for the onshore and offshore direction as the orbital motion of a water particle is assumed to be symmetric over the y-axis. Furthermore, it must be noted that the calculated velocities are based on the mean energy wave period and significant wave height. The grey line in Figure 4.22 represents the values were the calculated velocities are equal

to the maximum velocities. When the maximum measured velocities from the test are below this line, it can be concluded that the velocities are decreased inside the structure. This is a conservative approach as this is based on the mean energy wave period and significant wave height. In reality, the velocities are even decreased more.
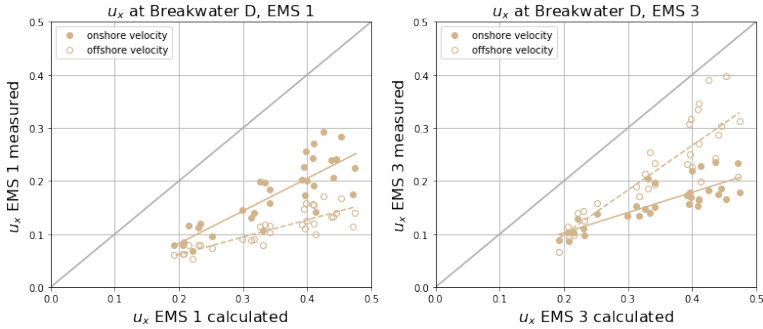
Figure 4.22: Measured and calculated horizontal orbital velocities for Breakwater D at EMS 1 and EMS3

From Figure 4.22 it can be concluded that Equation 4.8 does not give a good representation of the onshore and offshore horizontal orbital velocities inside the structure. The breakwater is causing the horizontal orbital velocity to decrease compared to the expected velocities outside the structure. Therefore, the space inside the structure can be seen as a possible shelter area for marine life.

For the onshore velocity at EMS 1, the measured orbital velocity is about 38% of the calculated horizontal orbital velocity outside the structure. For the onshore velocity at EMS 3, the measured velocity is about 61% of the calculated velocity outside the structure. The offshore velocity at EMS 1, is about 32% of the calculated velocity outside the structure. For the offshore velocity at EMS 3, the velocity in the breakwater is constantly about $0.1 m/s$ lower than calculated velocity outside the breakwater.

Lastly, at EMS 3 the highest velocities are measured. This is unexpected as at the lee side of the plate, a shadow zone is created what should result in lower flow velocities. However, probably the vertical impermeable plate is creating an eddy in the lee side of the structure that is causing these high offshore velocities.

5

DISCUSSION

In this chapter the uncertainties and limitations of this research are discussed. The main discussion points are; flume setup, 2D/3D, porosity.

Flume Setup For the setup of the flume different rules of thumb were used to define the dimensions of the model. During the data analysis an error was detected in the dimension of the foreshore. The length of the foreshore before the first wave gauge was too short. The length must be at least 2 times the wave length before the first wave gauge is placed. This is the length that is needed for the wave to adjust to the new water depth. In the model a length of 4.4 m was designed. But according to the rule of thumb, 13 m was needed.

To check the impact of this error on the results, the difference in measured wave height by WHM01 and WHM03 is calculated using the data of Breakwater C. In these tests the measured wave heights before the structure are less affected by the breakwater itself. A small difference in measured wave heights would indicate that the waves are adjusted to the new water depth. For most of the tests, this error ranged between 0 and 0.005 m. For a few tests, the error approached 0.01 m. These differences are small and therefore the short length of the foreshore does not affect the results and conclusions.

2D/3D In the wave flume only normally incident waves are tested. However in reality, submerged breakwaters experience waves from various directions. Therefore, not the full complexity of the processes is taken into account in this model. It is unclear how the permeability and porosity of the tested breakwaters would respond under oblique-wave attack. However, a two-dimensional wave flume is a good physical model to test the primary processes. From this, further research in a more complex environment could be done when deemed necessary.

Porosity   The area where the steel frame of Breakwater B was located is not taken into account for the calculation of the porosity. So, the mean porosity of the core may be slightly lower than the calculated porosity. However, the analysis shows that the performance of the permeable Breakwater B (n=0.44) compared to the impermeable Breakwater A (n=0) is rather similar, which indicates that small deviation from the applied porosity (n=0.44) are not likely to affect the conclusions. The same accounts for the perforated breakwaters were the surface porosity of the crest, diagonal, and vertical plate differ between respectively 0.44, 0.42 and 0.43. These small deviations are not likely to affect the conclusions as well.

6

CONCLUSION & RECOMMENDATIONS

In this chapter, the main conclusions from the thesis are discussed. With these conclusions the answer on the main research question is found. Resulting from this, recommendations for future research are proposed.

6.1. CONCLUSION

In this section, the (sub-) research questions which were stated in chapter 1 will be answered.

- **How can experiments in a flume be designed to obtain knowledge about the influence of permeability and porosity on the wave transmission of an artificial reef and its influence on the velocities inside the structure?**

  To study the influence of the permeability and porosity on the wave transmission of an artificial reef, five different breakwaters were tested in a two-dimensional wave flume at Deltares. For this, a scaling factor of 20 was applied. In all designs, a conventional trapezoidal-shape breakwater was tested. However, by changing the permeability, surface, and/or volume porosity, its influence on the wave transmission and orbital velocities could be investigated.

  First, a smooth impermeable breakwater (Breakwater A) was tested. For this structure, literature was available and therefore it functioned as the starting point for the other structures. Secondly, a rubble mound structure with a volume porosity of 0.44 (Breakwater B) was tested. Epoxy was used to fix the stones to guarantee constant permeability of the structure during the tests. Thirdly, a smooth perforated breakwater was designed with the same surface porosity as the volume porosity as Breakwater B (Breakwater C). This structure could identify possible effects of the volume porosity of a breakwater, as the surface porosity is still the same. Subsequently, a smooth perforated structure with a vertical impermeable screen in the

cross section was designed (Breakwater D). With this structure, it was investigated if solely the volume porosity, or also the permeability of the core were influencing the wave transmission. Lastly, a smooth perforated structure with a vertical perforated plate in the cross section (Breakwater E) was tested.

In total 208 tests were performed with different input variables for the wave height (H), wave steepness (S), wave period (T) and crest freeboard (R_c). The tests included breaking and non-breaking waves.

Before and after the structure, the wave heights were measured by two wave gauge sets to analyse the wave transmissions. At the perforated structures, also the horizontal orbital velocities inside the structure were measured by two or three EMSes. From this, the effect of the breakwater on the velocities inside the structure has been investigated as well.

- **What are the results of the physical model tests and how can they be interpreted?**

  (a) What are the wave transmissions of the tested models?

  In Table 6.1 the measured wave transmissions by the two wave gauge sets are presented.

	A	B	C	D	E
K_t	0.54-0.96	0.62-0.92	0.82-0.95	0.57-0.89	0.77-0.93

Table 6.1: Measured wave transmissions

Based on a detailed analysis, it can be concluded that Breakwater A, B, and D show similar wave transmissions. Breakwater E and C show higher wave transmissions as they dissipate less wave energy. This means that the core and permeability are of great influence on the wave transmission. Breakwater C and E are not useful as a breakwater as they dissipate little energy. However, by placing a vertical impermeable plate in the core at Breakwater C, which then becomes Breakwater D, there does occur a lot of wave dissipation, and therefore it can function as a coastal breakwater.

Furthermore, it is remarkable that Breakwater B shows mostly higher wave transmissions than Breakwater A, except for very low crests. van der Meer et al. (2005) suggested that rubble mound breakwaters should show lower wave transmissions than smooth impermeable breakwaters, as no wave dissipation at the crest, caused by the roughness and friction from the porosity, is present here. However, from the results, it can be concluded that the permeability of Breakwater B, that increases the wave transmission, overrules this suggestion by van der Meer et al. (2005). Therefore, resulting from this physical model, the hydraulic roughness and friction from the core can be assumed to be of less importance than the effects of the permeability on wave breaking.

(b) What is the influence of the relative crest freeboard (R_c/H_s), relative water depth (h/d), wave steepness (H_s/L), and relative crest width (B_c/L) on the wave transmission (K_t)?

R_c/H_s shows an exponential dependency on the wave transmission. Breakwater C and E show similar dependency and this dependency on R_c/H_s is lower than in Breakwater A, B and D. Breakwater B and D show similar dependency on R_c/H_s and Breakwater A shows the highest dependency.

All structures showed a linear dependency on H_s/L, h/H_s, and B_c/L although, for Breakwater C and E this dependency is negligible for all water depths. For Breakwater B and D there is little dependency on H_s/L, h/H_s, and B_c/L. Breakwater A shows the highest dependency on these dimensionless parameters, which increases with the water depth.

The influence of the water depth on the dependency of H_s/L, h/H_s, and B_c/L is hypothesised to be caused by the length of the waves and structure height that are causing some waves to move over the structure without 'feeling' the breakwater for larger water depths. Whereas, in shallow water, all waves will feel the structure and dissipate wave energy.

While in general Breakwater B and D show similar dependencies, it can be stated that for hollow breakwaters with a vertical screen, the surface porosity of the vertical screen mainly determines the behaviour of the breakwater.

(c) What is the influence of an artificial reef on the orbital velocities inside the structure?

For Breakwater C and E, no correlation was found between the horizontal orbital velocity and L, d, or H. For Breakwater D, there is a clear correlation between the orbital velocity and L and H. Therefore, only the velocities of Breakwater D were further analysed.

The maximum onshore velocity at EMS 1 is about 61% of the velocity outside the breakwater. At EMS 3 the onshore velocity is about 38% of the velocity outside the breakwater. At EMS 1 the maximum offshore velocity is about 32% of the velocity outside the breakwater and at EMS 3 the offshore velocity is constantly about $0.1 m/s$ lower than the velocity outside the structure. This zone (EMS 3) experiences the highest velocities of the structure.

It is remarkable that at EMS 3, which is at the lee side of the permeable breakwater with an impermeable screen, the highest velocities are measured. A shadow zone here is expected which should result in lower velocities than at EMS 1. Apparently, an eddy is formed that could explain these high velocities at EMS 3.

For Breakwater D, the marine snail, sea urchin and mussel can resist the storm conditions and therefore, Breakwater D can function as an artificial reef.

- **How do the measured wave transmissions from the physical model relate to the existing empirical formulas?**

The measured wave transmissions show a different dependency on R_c/H_s compared with existing empirical relations. The most remarkable difference is that in literature, by van der Meer (1990) and d'Angremond et al. (1996), a maximum wave transmission of 0.8 was set. Whereas in the physical model, wave transmissions close to 1.0 were measured. These results are physically more sound since for a very low structure that is not affecting the waves, the wave transmission coefficient should be 1. Moreover, it was expected that the impermeable breakwater (A) would result in higher wave transmission than the rubble mound breakwater (B), as no energy dissipation at the surface can occur according to van der Meer et al. (2005). However, from the experiment it was concluded that Breakwater A showed mostly lower wave transmissions than Breakwater B. Apparently the wave dissipation due to wave breaking above the structure becomes less for permeable structures.

When looking at the existing empirical relations for the wave transmission over a submerged breakwater, at the moment, the following literature predicts the wave transmission the best; Breakwater A: van der Meer (1990), Breakwater B and D: d'Angremond et al. (1996) formula for permeable structures, and Breakwater E and C: Bleck and Oumeraci (2001).

From this, it can be concluded that there is no single empirical relation that correctly predicts the wave transmission for Breakwaters A, B, and D that showed similar wave transmissions.

- **Can a new empirical relation for the wave transmission over artificial coastal reefs be derived from the physical model results?**

From the physical model it was concluded that Breakwater A, B, and D showed similar wave transmissions and Breakwater B and D showed similar dependencies on the dimensionless parameters. Therefore, it was decided to derive a new formula for Breakwater A, B and D as there is no existing empirical relation that correctly describes the wave transmission for these breakwaters.

From the physical model results it was concluded that R_c/H_s showed the most influence on the wave transmission. However, an empirical relation that only took R_c/H_s into account, had still a too large RMSE. Therefore, the influence of h/H_s was also taken into account. This resulted in the following equation following from a multiple regression analysis:

$$K_t = -0.59 \cdot e^{\frac{R_c}{H_s}} - 0.042 \frac{h}{H_s} + 1.12 \tag{6.1}$$

This equation showed an RMSE of 0.032 based on the wave transmissions of A, B, and D. An RMSE of 0.040 was found for Breakwater A, 0.031 for Breakwater B and 0.023 for Breakwater D respectively. These RMSEs show that the new empirical expression performs better than all existing empirical expressions.

The answers to these sub-questions are now used to the answer of the main research question of this master thesis:

How do the permeability and the porosity of an artificial coastal reef influence wave transmission and the sheltered habitat of marine life?

For a perforated hollow breakwater, adding an impermeable plate in the cross section results in similar wave transmissions as a rubble mound breakwater and a smooth permeable structure with a vertical screen. From this, it is concluded that for hollow permeable breakwaters wit a vertical screen inside, the surface porosity of this vertical screen determines the wave transmission.

For artificial reefs, hollow perforated-type structures provide the desired hydrodynamic behaviour. This newly obtained knowledge could affect the future design of artificial reefs.

Prior to the present research, it was believed that the best coastal protection is achieved by breakwaters that are smooth and impermeable. But in this research it was discovered that a hollow, perforated structure can achieve a wave transmission that is almost as low as transmission of a smooth, impermeable structure when an impermeable screen is placed in its middle. This means that a hollow, perforated structure can act as both an artificial reef that provides a safe habitat for marine life, and as a breakwater that provides sufficient coastal protection.

For the design of such breakwaters, newly derived Equation 6.1 can be used. This formula is valid for smooth impermeable breakwaters, permeable rubble mound breakwaters, and hollow impermeable perforated breakwaters.

Furthermore, an hollow perforated breakwater with an impermeable vertical screen inside decreases the horizontal orbital velocity inside the structure. The impermeable screen in the middle of the structure divides the hollow structure into two parts: the part on the lee side of this screen shows the highest velocities which are in offshore direction. The velocities inside the structure are low enough for marine life to withstand storm conditions, and therefore the function of an artificial reef, which is creating a sheltered habitat for marine life, is still guaranteed.

6.2. RECOMMENDATIONS

With the knowledge obtained from the results and experiments of this master thesis, some recommendations are made for further research.

- **Investigate other surface porosities for a hollow perforated breakwater with an impermeable screen**
  In this thesis it was concluded that the impermeable screen for a hollow perforated breakwater is causing the decrease in wave transmission. The perforated outer layer is thought to define the characteristic dependencies of the breakwater and the influence on the velocities inside the structure. It is recommended to perform more physical model tests with different surface porosities for this outer layer, as this could confirm that even with a porosity higher than 0.44 (even approaching 1), still enough wave dissipation is achieved. Moreover, its influence on the velocities inside the structure can then be further investigated. With this knowledge, the surface porosity could be adapted to the required velocities for the marine life that the artificial reef needs to attract. Knowing that an impermeable screen inside the structure would result in enough wave dissipation would give reef designers more freedom to focus on the ecological aspects of the structure. Even changing the surface porosities over the length of the breakwater then becomes an option, which could create the conditions to have different marine life communities in one breakwater.

- **Investigate the wave transmissions and velocities inside the structure for submerged perforated breakwaters with multiple impermeable screens**
  The placement of an impermeable screen in the middle of a perforated hollow breakwater caused a significant decrease in wave transmission. By placing multiple impermeable screens inside the structure, more spaces inside the structure are created that may result in an extra decrease of the wave transmission as the orbital motion is blocked even more. This will also influence the velocities inside the structure, as now more different hydraulic environments are created which might provide additional advantages for marine life.

- **Investigate the effect of a perforated impermeable breakwater on the morphology around the structure**

  In this research, solely the hydraulic performance of artificial reefs has been investigated. Breakwater D, the perforated hollow structure, showed low wave transmissions and velocities inside the structure. However, the effect on the morphology and scour at the toe of the structure has not been investigated. As the impermeable screen is blocking the cross-shore transport, it could happen that the impermeable screen is causing scour and/or sedimentation inside the structure that will consequently influence the space and velocities inside the structure. The indication of the presence of an eddy would also suggest that inside the structure, scour could be present. Further research should determine its influence on the stability of the structure and marine life in the artificial reef. In this research, different locations of the perforations and different surface porosities could be tested. Following from

this research, the locations and amount of perforations could be optimized for the morphology inside and around the structure.

REFERENCES

Armono, H. D. (2004). *Artificial Reefs as Shoreline Protection Structures Related papers* (tech. rep.).

Bleck, M., & Oumeraci, H. (2001). *Wave Dampening and Spectral Evolution at Artificial Reefs* (tech. rep.). Leichtweiß-Institute for Hydraulic Engineering.

Bohnsack, J. A. (1998). *Are High Densities of Fishes at Artificial Reefs the Result of Habitat Limitation or Behavioral Preference?* (Tech. rep.).

Bohnsack, J. A., & Sutherland, D. L. (1985). *Artificial Reef Research: A Review with Recommendations for Future Priorities* (tech. rep. No. 1).

Briganti, R., Van Meer, J. D., Buccino, M., & Calabrese, M. (2003). Wave transmission behind low-crested structures. *Coastal Structures 2003 - Proceedings of the Conference*, 580–592. https://doi.org/10.1061/40733(147)48

Buccino, M., & Calabrese, M. (2007). Conceptual Approach for Prediction of Wave Transmission at Low-Crested Breakwaters. https://doi.org/10.1061/ASCE0733-950X2007133:3213

Calabrese, M., Vicinanza, D., & Buccino, M. (2002). *Low-Crested and Submerged Breakwaters in Presence of Broken Waves* (tech. rep.). University of Naples Federico II and second University of Naples. Naples.

Cardenas-Rojas, D., Mendoza, E., Escudero, M., & Verduzco-Zapata, M. (2021). Assessment of the performance of an artificial reef made of modular elements through small scale experiments. *Journal of Marine Science and Engineering, 9*(2), 1–18. https://doi.org/10.3390/jmse9020130

CIRIA, CUR, & CETMEF. (2012). The Rock Manual. The use of rock in hydraulic conditions (2nd edition), 306–468.

Daemen, I. (1991). *Wave transmission at low-crested structures* (tech. rep.). Delft University of Technology.

d'Angremond, K., van der Meer, W., Jentsje, W., & de Jong, R. (1996). *Wave Transmission At Low-Crested Structures* (tech. rep.). Coastal Engineering Proceedings.

Deltares. (n.d.). Instrument, Wave height meter. www.deltares.nl

Eco-solutions – Reefy. (n.d.). https://reefy.nl/tailored-eco-solutions/

Friebel, H. C., & Harris, L. (2003). *Re-evaluation of Wave Transmission Coefficient Formulae from Submerged Breakwater Physical Models* (tech. rep.).

Gerrit, S. J., & Verhagen, H. J. (2016). *Introduction to Bed, bank and shore protection* (2nd, Vol. 413). Delft Academic Press.

Heller, V. (2011). Scale effects in physical hydraulic engineering models. *Journal of Hydraulic Research, 49*(3), 293–306. https://doi.org/10.1080/00221686.2011.578914

Hoegh-Guldberg, O., Mumby, P. J., Hooten, A. J., Steneck, R. S., Greenfield, P., Gomez, E., Harvell, C. D., Sale, P. F., Edwards, A. J., Caldeira, K., Knowlton, N., Eakin, C. M., Iglesias-Prieto, R., Muthiga, N., Bradbury, R. H., Dubi, A., & Hatziolos,

M. E. (2007). Coral reefs under rapid climate change and ocean acidification. *Science (New York, N.Y.), 318*(5857), 1737–1742. https://doi.org/10.1126/science.1152509

Hoegh-Guldeberg, O. (2010). Coral reef ecosystems and anthropogenic climate change. *Springer*. https://doi.org/10.1007/s10113-010-0189-2

Holthuijsen, L. H. (2007). *Waves in Oceanic and Coastal Waters*. Cambridge University Press, New York.

Hughes, S. A. (1993). Physical models and laboratory techniques in coastal engineering, 568.

Hughes, T. P., Baird, A. H., Bellwood, D. R., Card, M., Connolly, S. R., Folke, C., Grosberg, R., Hoegh-Guldberg, O., Jackson, J. B. C., Kleypas, J., Lough, J. M., Marshall, P., Nyström, M., Palumbi, S. R., Pandolfi, J. M., Rosen, B., & Roughgarden, J. (2003). Climate Change, Human Impacts, and the Resilience of Coral Reefs. www.sciencemag.org

Hughes, T. P., Kerry, J. T., Baird, A. H., Connolly, S. R., Chase, J., Dietzel, A., Hill, T., Hoey, A. S., Hoogenboom, M. O., Jacobson, M., Kerswell, A., Madin, J. S., Mieog, A., Paley, A. S., Pratchett, M. S., Torda, G., & Woods, M. (1996). Global warming impairs stock-recruitment dynamics of corals, 43–44. https://doi.org/10.1038/s41586-019-1081-y

Ibrahim, I. N., Razak, M. S. A., Yusof, B., & Desa, S. M. (2020). The performance of narrow and broad-crested submerged breakwaters in dissipating wave heights. *Jurnal Teknologi, 82*(3), 25–33. https://doi.org/10.11113/jt.v82.13974

Kirkegaard, J., Wolters, G., Sutherland, J., Soulsby, R., Frostick, L., McLelland, S., Mercer, T., & Gerritsen, H. (2011). *Users Guide to Physical Modelling and Experimentation, Experience of the HYDRALAB Network* (tech. rep.). CRC Press/Balkema. Leiden. www.iahr.org

Koutandos, E., Koutitas, C., & Prinos, P. (2006). *Permeability Effects On Breaking Waves Over Submerged Rubble Mound Breakwaters*. Drexel university.

Kuang, C., Mao, X., Gu, J., Niu, H., Ma, Y., Yang, Y., Qiu, R., & Zhang, J. (2019). Morphological processes of two artificial submerged shore-parallel sandbars for beach nourishment in a nearshore zone. *Ocean & Coastal Management, 179*, 104870. https://doi.org/10.1016/J.OCECOAMAN.2019.104870

Le Xuan, T., Le Manh, H., Ba, H. T., Van, D. D., Duong Vu, H. T., Wright, D., Bui, V. H., & Anh, D. T. (2022). Wave energy dissipation through a hollow triangle breakwater on the coastal Mekong Delta. *Ocean Engineering, 245*. https://doi.org/10.1016/j.oceaneng.2021.110419

Lemoine, H. R., Paxton, A. B., Anisfeld, S. C., Rosemond, R. C., & Peterson, C. H. (2019). Selecting the optimal artificial reefs to achieve fish habitat enhancement goals. *Biological Conservation, 238*, 108200. https://doi.org/10.1016/J.BIOCON.2019.108200

Lokesha, Sannasiraj, S. A., & Sundar, V. (2019). Hydrodynamic characteristics of a submerged trapezoidal artificial reef unit. *Proceedings of the Institution of Mechanical Engineers Part M: Journal of Engineering for the Maritime Environment, 233*(4), 1226–1239. https://doi.org/10.1177/1475090218825178

Ma, Y., Kuang, C., Han, X., Niu, H., Zheng, Y., & Shen, C. (2020). Experimental study on the influence of an artificial reef on cross-shore morphodynamic processes of a wave-dominated beach. *Water*, *12*(10), 1–28. https://doi.org/10.3390/w12102947

Mahmoudi, A., Hakimzade, H., Ketabdari, M. J., Cartwright, N., & Vaghefi, M. (2017). *Experimental Study on Wave Transmission and Reflection at Impermeable Submerged Breakwaters* (tech. rep. No. 3). http://ijcoe.org/browse.php?a_code=A-10-80-1&sid=1&slc_lang=en

Makris, C., & Memos, C. D. (2007). *Wave Transmission over Submerged Breakwaters: Performance of Formulae and Models*. International Society of Offshore; Polar Engineers.

MARS — Reef Design Lab. (n.d.). https://www.reefdesignlab.com/mars1

MOSES / Solutions | ReefSystems. (n.d.). https://www.reefsystems.org/moses

Na'Im, I. I., Shahrizal, A. R. M., & Safari, M. D. (2018). A Short Review of Submerged Breakwaters. *MATEC Web of Conferences*, *203*. https://doi.org/10.1051/matecconf/201820301005

Pilarczyk, K. W. (2003). *Design of low-crested (submerged) structures-an overview* (tech. rep.). Delft University of Technology.

Profile, S., Memos, C. D., Kontaxi, C., & Memos, C. (2005). *Submerged Breakwaters as Artificial Habitats* (tech. rep.).

Scheldt Flume - Deltares. (n.d.). https://www.deltares.nl/nl/faciliteiten/scheldegoot/

Seabrook, S. R., & Hall, K. R. (1998). *Wave Transmission at Submerged Rubblemound Breakwaters* (tech. rep.).

Sharif Ahmadian, A. (2016). Fundamental Concepts. *Numerical Models for Submerged Breakwaters*, 17–27. https://doi.org/10.1016/B978-0-12-802413-3.00002-X

Sidek, F. J., Al-Jeffry, M., & Wahab, A. (2007). *The Effects of Porosity Of Submerged Breakwater Structures on Non-Breaking Wave Transformations* (tech. rep. No. 1).

Sollitt, C. K., & Cross, R. H. (1972). *Wave Transmission Through Permeable Breakwaters* (tech. rep.).

United Nations. (2017). *Factsheet: People and Oceans* (tech. rep.). United Nations. New York.

van der Meer, J. W., Regeling, H. J., & De Waal, J. P. (2000). Wave transmission: spectral changes and its effects on run-up and overtopping.

van der Meer, J. W. (1990). *Data on Wave Transmission due to overtopping* (tech. rep.). Delft Hydraulics report no. H 986, prepared for CUR C67.

van der Meer, J. W., Briganti, R., Zanuttigh, B., & Wang, B. (2005). Wave transmission and reflection at low-crested structures: Design formulae, oblique wave attack and spectral change. *Coastal Engineering*, *52*(10-11), 915–929. https://doi.org/10.1016/j.coastaleng.2005.09.005

van der Meer, J. W., & Daemen, I. F. R. (1994). *Stability and Wave Transmission at Low-Crested and Rubble-Mound Structures* (tech. rep.).

van Gent, M. R. A. (1999). Wave run-up and wave overtopping for double peaked wave energy spectra. *Delft Hydraulics Report H3351*.

van Gent, M. R. A. (2001). Wave Runup on Dikes with Shallow Foreshores. *Journal of Waterway, Port, Coastal, and Ocean Engineering, 127*(5), 254–262. https://doi.org/10.1061/(ASCE)0733-950X(2001)127:5(254)

WWF. (2004). Cold-water corals. *12*, 1–12.

Yalin, M. S. (1971). *Theory of Hydraulic Models*. The Macmillan Press LTD.

Yincan et al, Y. (2017). Coastal Erosion. *Marine Geo-Hazards in China*, 269–296. https://doi.org/10.1016/B978-0-12-812726-1.00007-3

A

TEST INPUT

Every breakwater is tested with 4 wave heights, 2 wave steepness's and 4 water depths. For Breakwater C and E, also additional emerged conditions are tested.

Test ID	Parameter	Test input	Structure
$SXXX$	$S_{m-1,0}$	0.02, 0.04	A, B, C, D, E
$XdXX$	$d[m]$	0.25, 0.30, 0.35, 0.40, 0.45, 0.50	C, E
		0.35, 0.40, 0.45, 0.50	A, B, D
XXR_cX	$R_c[m]$	0.05, 0, -0.05, -0.10, -0.15, -0.20	C, E
		-0.05, -0.10, -0.15, -0.20	A, B, D
$XXXH$	$H_{m0}[m]$	0.10, 0.15, 0.20	C, E
		0.10, 0.15, 0.20, 0.25	A, B, D

Table A.1: Experiment input

The test IDs have the following meaning;

- S: $[1,2] = [0.02, 0.04]$

- d: $[4,5,0,1,2,3] = [0.25, 0.30, 0.35, 0.40, 0.45, 0.50]$

- R_c: $[4,5,0,1,2,3] = [0.05, 0, -0.05, -0.10, -0.15, -0.20]$

- H: $[1,2,3,4] = [0.10, 0.15, 0.20, 0.25]$

Test	Sm-1,0	d	Rc	Hm0	Tm-1,0	Tp	Lm	Lp
1551	0,02	0,3	0	0,10	1,79	1,98	3,07	3,40
1552	0,02	0,3	0	0,15	2,19	2,43	3,76	4,16
1553	0,02	0,3	0	0,20	2,53	2,80	4,34	4,80
2551	0,04	0,3	0	0,10	1,26	1,40	2,17	2,40
2552	0,04	0,3	0	0,15	1,55	1,71	2,66	2,94
2553	0,04	0,3	0	0,20	1,79	1,98	3,07	3,40
1441	0,02	0,25	0,05	0,10	1,79	1,98	2,80	3,10
1442	0,02	0,25	0,05	0,15	2,19	2,43	3,43	3,80
1443	0,02	0,25	0,05	0,20	2,53	2,80	3,96	4,39
2441	0,04	0,25	0,05	0,10	1,26	1,40	1,98	2,19
2442	0,04	0,25	0,05	0,15	1,55	1,71	2,43	2,69
2443	0,04	0,25	0,05	0,20	1,79	1,98	2,80	3,10
1001	0,02	0,35	-0,05	0,10	1,79	1,98	3,31	3,67
1002	0,02	0,35	-0,05	0,15	2,19	2,43	4,06	4,49
1003	0,02	0,35	-0,05	0,20	2,53	2,80	4,69	5,19
1004	0,02	0,35	-0,05	0,25	2,83	3,13	5,24	5,80
2001	0,04	0,35	-0,05	0,10	1,26	1,40	2,34	2,59
2002	0,04	0,35	-0,05	0,15	1,55	1,71	2,87	3,18
2003	0,04	0,35	-0,05	0,20	1,79	1,98	3,31	3,67
2004	0,04	0,35	-0,05	0,25	2,00	2,21	3,71	4,10
1111	0,02	0,4	-0,1	0,10	1,79	1,98	3,54	3,92
1112	0,02	0,4	-0,1	0,15	2,19	2,43	4,34	4,80
1113	0,02	0,4	-0,1	0,20	2,53	2,80	5,01	5,55
1114	0,02	0,4	-0,1	0,25	2,83	3,13	5,60	6,20
2111	0,04	0,4	-0,1	0,10	1,26	1,40	2,51	2,77
2112	0,04	0,4	-0,1	0,15	1,55	1,71	3,07	3,40
2113	0,04	0,4	-0,1	0,20	1,79	1,98	3,54	3,92
2114	0,04	0,4	-0,1	0,25	2,00	2,21	3,96	4,39
1221	0,02	0,45	-0,15	0,10	1,79	1,98	3,76	4,16
1222	0,02	0,45	-0,15	0,15	2,19	2,43	4,60	5,10
1223	0,02	0,45	-0,15	0,20	2,53	2,80	5,31	5,88
1224	0,02	0,45	-0,15	0,25	2,83	3,13	5,94	6,58
2221	0,04	0,45	-0,15	0,10	1,26	1,40	2,66	2,94
2222	0,04	0,45	-0,15	0,15	1,55	1,71	3,25	3,60
2223	0,04	0,45	-0,15	0,20	1,79	1,98	3,76	4,16
2224	0,04	0,45	-0,15	0,25	2,00	2,21	4,20	4,65
1331	0,02	0,5	-0,2	0,10	1,79	1,98	3,96	4,39
1332	0,02	0,5	-0,2	0,15	2,19	2,43	4,85	5,37
1333	0,02	0,5	-0,2	0,20	2,53	2,80	5,60	6,20
1334	0,02	0,5	-0,2	0,25	2,83	3,13	6,26	6,93
2331	0,04	0,5	-0,2	0,10	1,26	1,40	2,80	3,10
2332	0,04	0,5	-0,2	0,15	1,55	1,71	3,43	3,80
2333	0,04	0,5	-0,2	0,20	1,79	1,98	3,96	4,39
2334	0,04	0,5	-0,2	0,25	2,00	2,21	4,43	4,90

B

CONSTRUCTION BREAKWATERS B, C, D, AND E

B.1. BREAKWATER B

For the construction of the rubble mound breakwater it is important that the stones do not move to keep the permeability constant during the tests. To prevent the stones from moving, epoxy is used to fix the stones to each other. Moreover, a steel frame is constructed inside the structure which is necessary for the transportation of the breakwater to the flume. In Figure B.1 different stages of the construction of Breakwater B are presented.
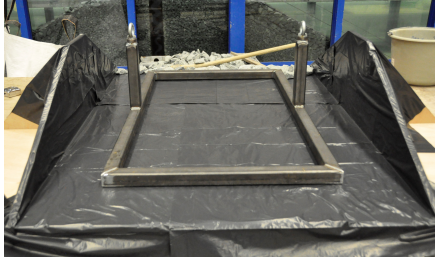
(a) The wooden mold and a steal frame of the breakwaters

(b) First layer of stones in the mold

(c) First layers of stones fixed with epoxy

(d) Final stage of the breakwater in the mold

Figure B.1: Construction rubble mound breakwater, Breakwater B

In Figure B.2 the final stage is presented.

Figure B.2: Rubble mound breakwater, Breakwater B

B.1.1. POROSITY

The porosity is the volume of voids compared to the total volume of the structure. To calculate the exact porosity of Breakwater B, first the self-weight of the stones is determined. This is done by measuring the volume and weight of the water before and after placing stones in it. To get a reliable result, this is repeated five times. This resulted in a self-weight of 2707.3 kg/m^3. The measurements are presented in Table B.1.

Sample	Above water [gr]	Below water [gr]	Volume [dm3]	ρ[kg/m3]
1	1935.9	1222.5	713.4	2713.62
2	2262.6	1428.7	833.9	2713.27
3	2347.4	1477.6	869.8	2698.78
4	1717.5	1083.0	634.5	2706.86
5	2096.3	1321.0	775.3	2703.86
			Average	2707.28

Table B.1: Calculation self-weight of the rubble mound rocks

For the calculation of the porosity of the breakwater, the volume and weight of the steel frame is not taken into account. Using the values from Table B.2 and Table B.1, the porosity of Breakwater B is calculated.

Volume breakwater [m^3]	0.23856
Volume steel frame [m^3]	0.006016
Volume structure with rocks [m^3]	0.232544
Weight structure [kg]	377
Weight steel frame [kg]	12.5
Weight structure with rocks [kg]	364.5
Self-weight rocks [kg/m^3]	2.7073
Volume stones [m^3]	0.1346
Volume voids[m^3]	0.1039
Porosity	0.4356

Table B.2: Calculation porosity rubble mound breakwater

$$n = \frac{V_p}{V_t} = \frac{0.1039}{0.2385} = 0.4356 \tag{B.1}$$

B.2. BREAKWATER C

To get the same surface porosity as the volume porosity of Breakwater B, 232 holes with a diameter of 4 cm and 2 holes with a diameter of 5 cm are drilled in the diagonal plate. This resulted in a surface porosity of 0.443. For the crest plate, 64 holes with a diameter of 4 cm and two holes with a diameter of 5 cm are drilled. This resulted in a surface porosity of 0.424. The two holes of 5 cm are needed to be able to place the EMS inside the structure while the diameter of an EMS is exactly 4 cm.
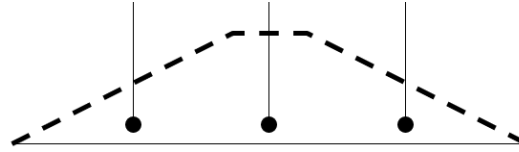
(a) Cross-section Breakwater C
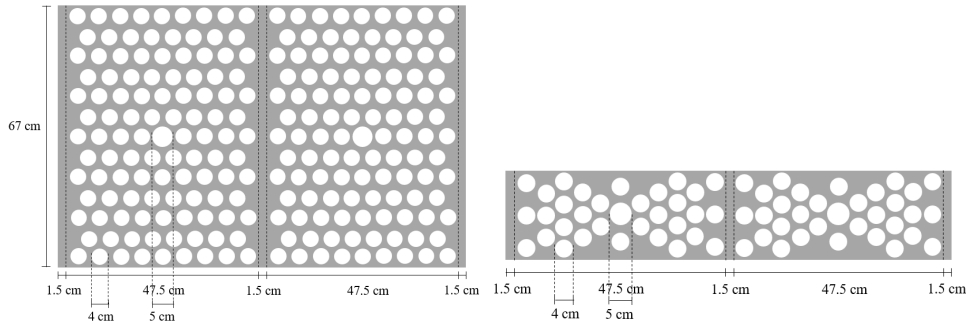
(b) Diagonal plate Breakwater C

(c) Crest plate Breakwater C

Figure B.3: Dimensions design of Breakwater C

B.3. BREAKWATER D

For Breakwater D, the same diagonal and crest plate as for Breakwater C are used. Therefore, also here, the surface porosity of the diagonal plate (0.443) and crest plate (0.424) are the same. Additionally, a vertical impermeable plate is placed in the middle of the cross section.
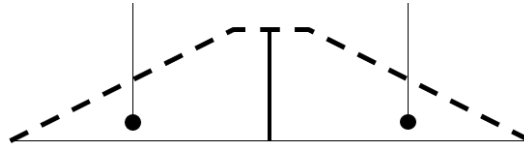
(a) Cross-section Breakwater D
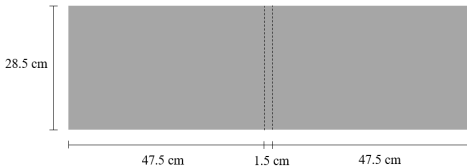
(b) Vertical plate Breakwater D
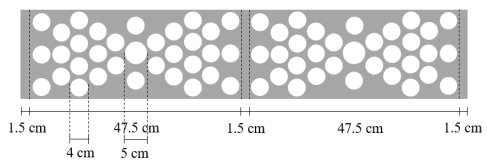
(c) Crest plate Breakwater D
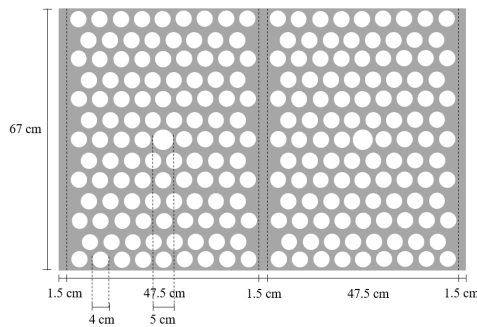
(d) Diagonal plate Breakwater D

Figure B.4: Dimensions design of Breakwater D

B.4. BREAKWATER E

For Breakwater E, the same diagonal and crest plates from Breakwater C are used as well. This results again in a surface porosity of 0.443 for the diagonal plate and a surface porosity of 0.424 for the crest plate. Furthermore, a vertical perforated plate is located in the middle of the breakwater with a surface porosity of 0.425.

(a) Cross-section Breakwater D

(b) Vertical plate Breakwater E

(c) Crest plate Breakwater E

(d) Diagonal plate Breakwater E
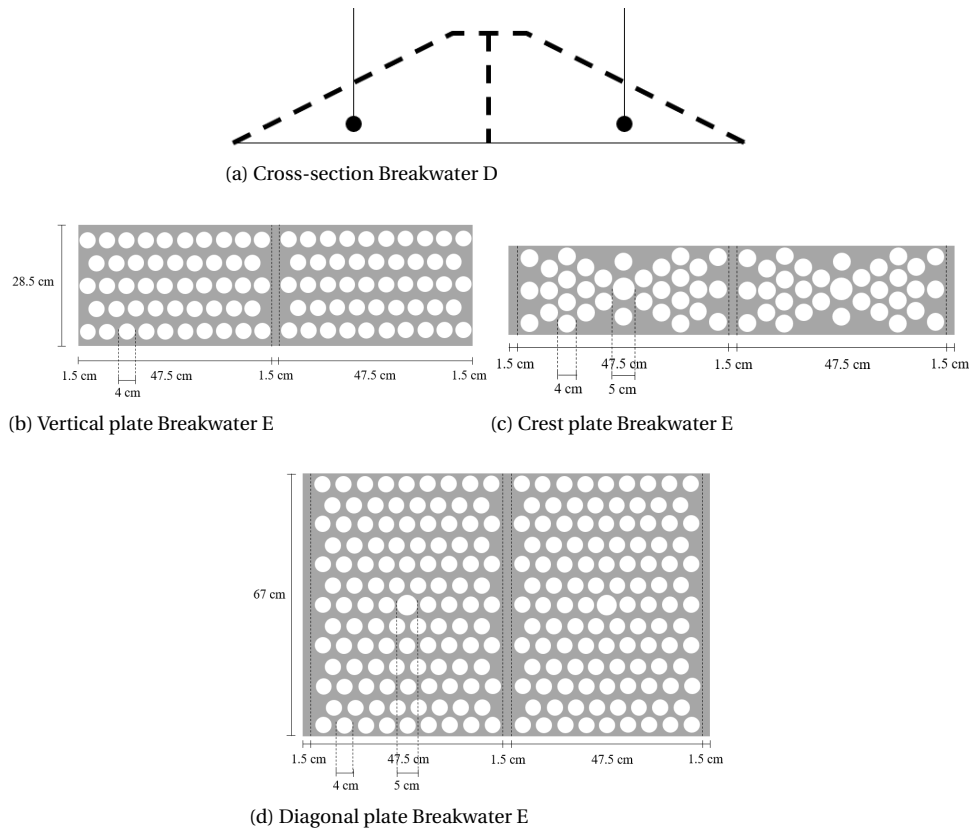
Figure B.5: Dimensions design of Breakwater E

C

INSTRUMENTATION

C.1. Wave Height Meter

Before and after the breakwater, three Wave Height Meters (WHM) are located to record the free surface elevation. The distance between these meters is dependent on the test-input and was calculated by Deltares. Figure C.1 gives an impression of the wave gauges during the experiment.

The probe of the meter is constructed with two parallel stainless steel rods which are mounted underneath a box, perpendicular to the flow direction. These rods act as the electrodes of this box. A platinum reference electrode is included to compensate for the varying electrical conductivity of the fluid. When the water level is varying, so is the electrical conductivity signal. The output signal is linearly proportional to the liquid level and instrument voltage (Deltares, n.d.).

It is important that the robs are re-calibrated every time the water level is changed in order to stay in the voltage range of the rods. Furthermore, during the experiments, it is important that the robs are submerged under all conditions.

(a) Position wave height meter in cross-section

(b) Wave gauge set in action

Figure C.1: WHM physical model

C.2. Electromagnetic Liquid Velocity Meter

For Breakwater C, D and E, also the horizontal velocities inside the structure are measured. This is done by placing 2 or 3 electromagnetic liquid velocity meters (EMSes). Figure C.2 gives an impression of the velocity meters during the experiment. An EMS can measure the bi-directional water velocity in two perpendicular directions. It measures the water velocity by the principle of conductive liquid moving through a magnetic field. This field is induced by an electrical current in a small coil inside the probe. The probe is designed such that the measured voltages are proportional to the liquid velocity parallel to the plane of the electrodes (Deltares, n.d.).

In the physical model, only the velocities in the horizontal direction will differ. The velocities over the width of the flume are constant. Therefore, only one measured velocity can be used in the data-analysis whereas two velocities are measured.
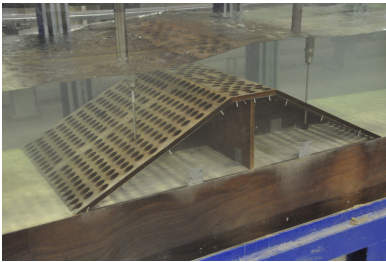
(a) EMS in action for Breakwater D
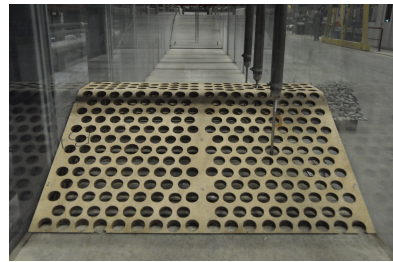
(b) Position of the EMS over the cross-section

Figure C.2: EMS in a breakwater

D

WAVE SPECTRUM

For the analysis of the wave spectrum, the raw data of the experiments is used. For calculating the incoming and transfered wave spectra, the mean of the measured wave heights at WHM01, WHM02, and WHM03 together with fourier transformation is used to calculate the incoming wave spectra. The mean of the measured wave heights by WHM04, WHM05, WHM06 is used to calculate the outcoming wave spectra. Because the raw data is used, reflection of the breakwater and wave absorber is not taken into account. This will lead to some errors in the calculated mean and peak wave period compared with the measured mean and peak wave period.

In Figure D.1 the changes in the wave spectra for test 2112 (s = 0.04, d = 40 cm, R_c = 0.10 cm, H = 0.15 cm) are presented. In Figure D.2 the changes in the wave spectrum for test 2002 (s=0.04, d = 0.35, Rc = 0.05, H = 0.15) are presented. From Figure D.1 and D.2 it can be concluded that the peak period barerly changed, meaning that the peak of the wave energy in the spectrum stays the same. For breakwater A, B, and D, the transferred mean period ($T_{m-1,0}$) is decreased which results in a shift to the higher frequencies in the spectrum. Whereas for Breakwater C and D, the transferred mean period is increased meaning a shift to the lower frequency in the spectra.

From Figure D.1 and D.2 the differences in wave transmission are also visible. The peak of the wave spectrum for Breakwater A, B, and D is lower than for Breakwater C and D.
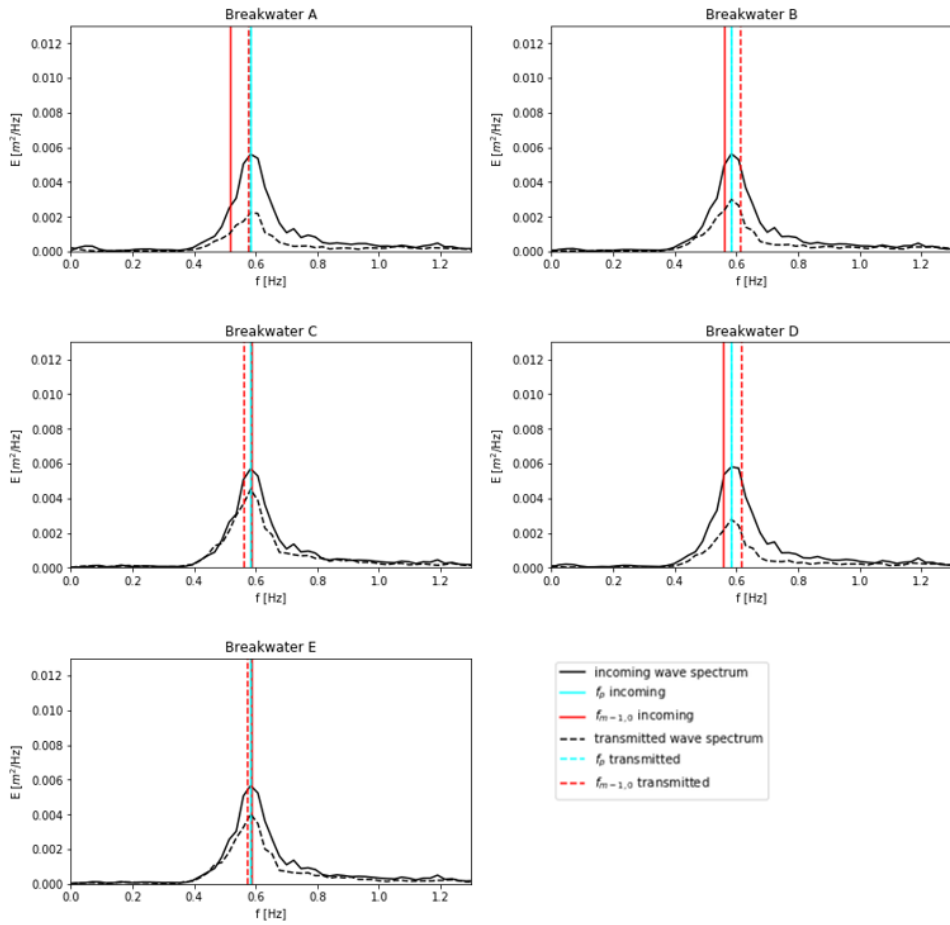
Figure D.1: Wave spectrum changes test 2112
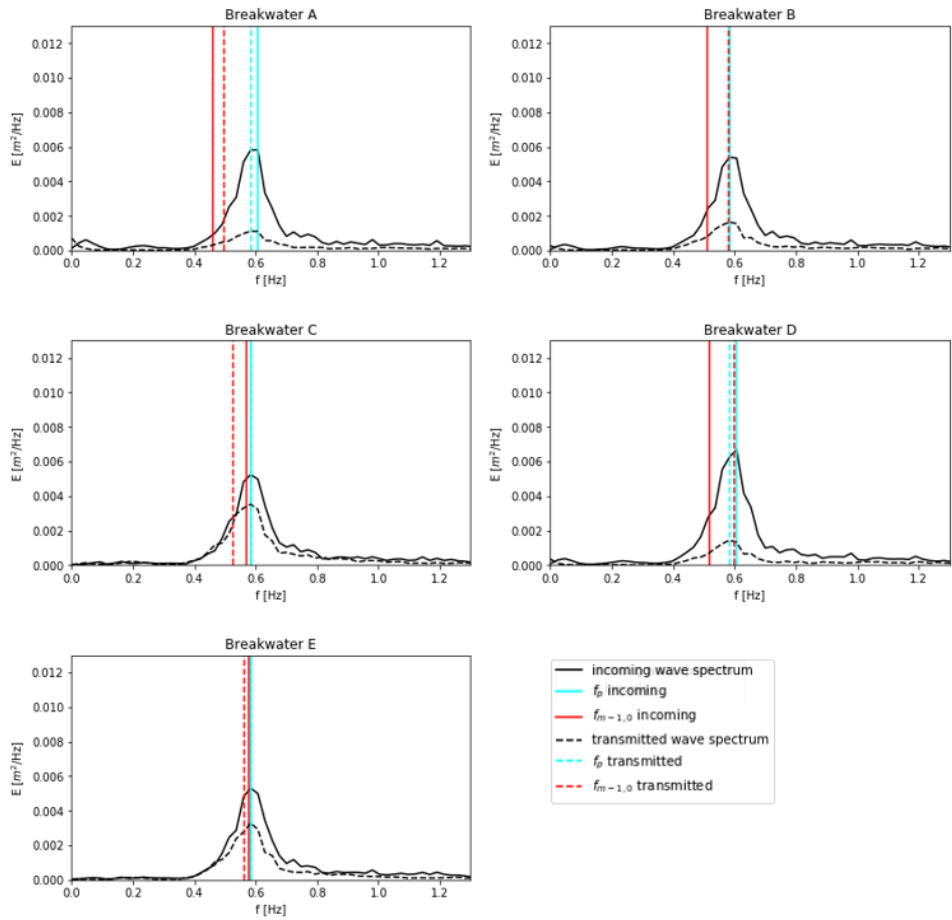
Figure D.2: Wave spectrum changes test 2002

In Figure D.3 changes in the wave spectra for test 1004 (s = 0.02, d = 0.35 cm, R_c = 0.05, H = 0.25 cm) are presented. Due to wave breaking already in front of the breakwater, a peak at the lower frequencies is observed. This is caused by depth-induced wave breaking before the first wave gauge. Here, the water depth is too low to reach a wave height of 0.25 cm.

From Figure D.3 it can observed that the peak frequencies stays the same. The transmitted mean period for all breakwaters, except Breakwater C, is decreased. This indicates a transfer to the higher frequencies in the wave spectra.

Moreover, it can be observed that for Breakwater A, B, and D, the higher frequencies are cut. For Breakwater B this is probably caused by flow through the breakwater. For Breakwater A and D, this is probably caused by the impermeability of the structure.
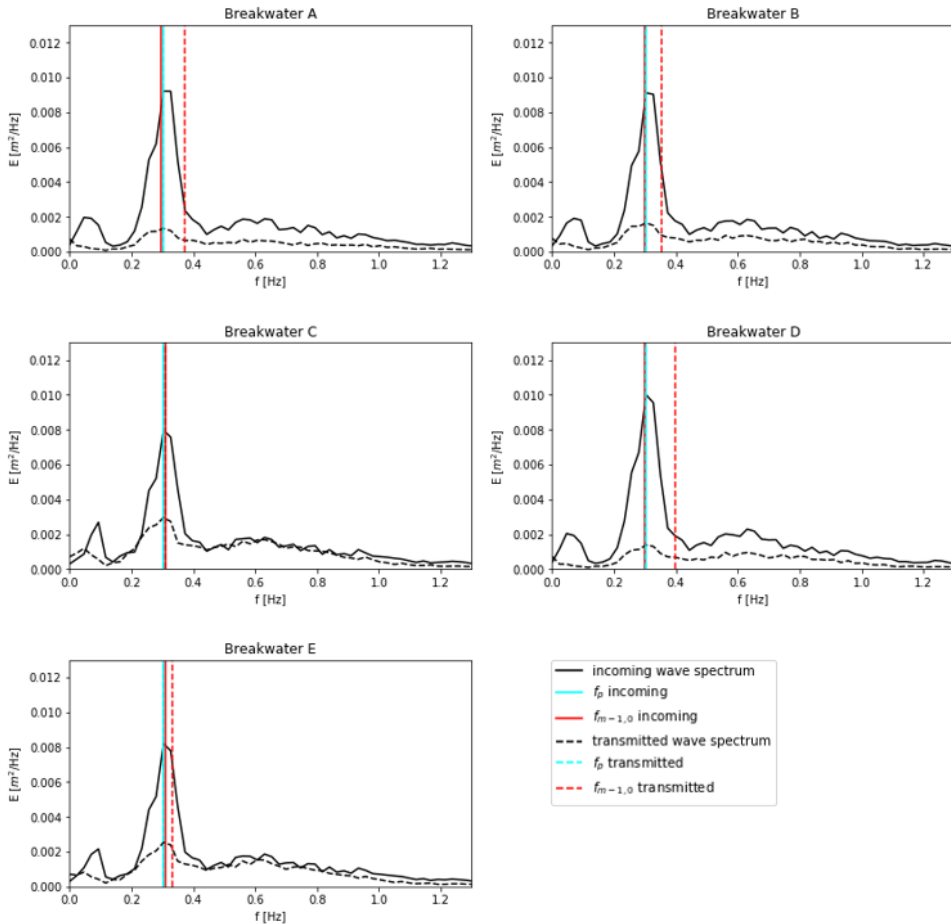
Figure D.3: Wave spectrum changes test 1004

In Figure D.4 changes in the wave spectrum for test 1331 (s=0.02, d = 0.50 cm, R_c = 0.10 cm, H = 0.10 cm) are presented. As a high wave transmission was calculated for this test, also little changes in the wave spectra can be observed.
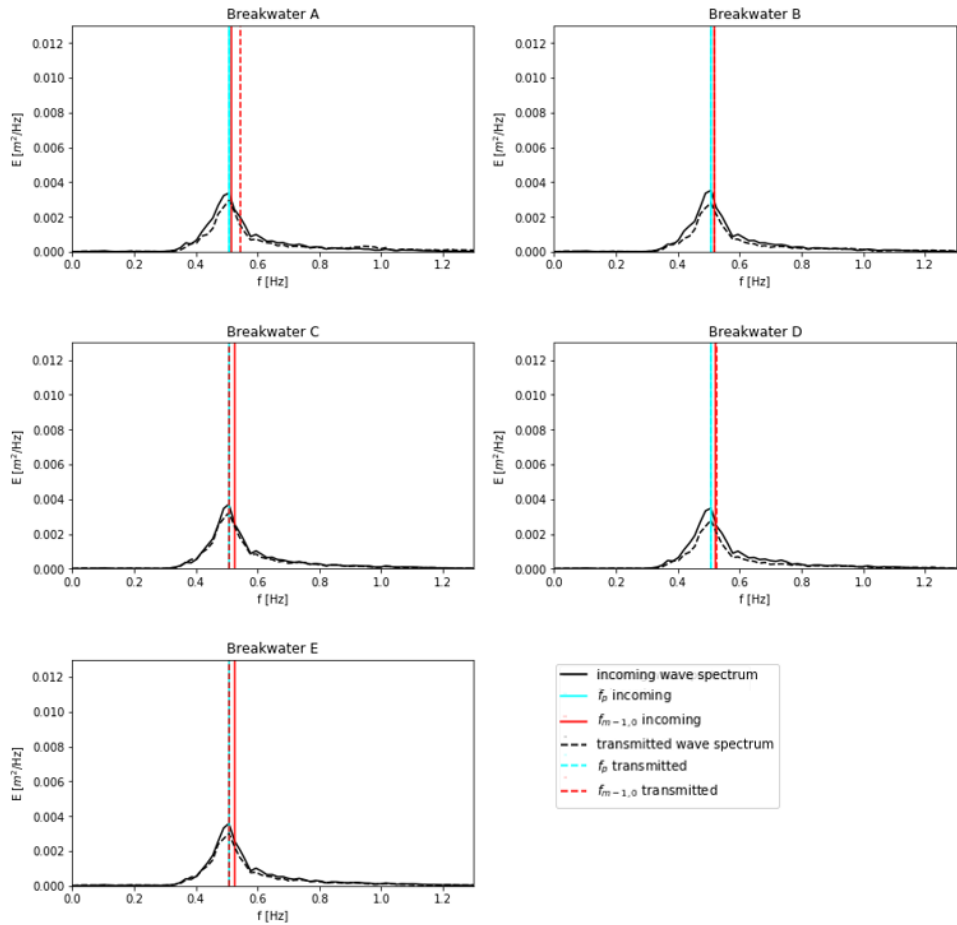
Figure D.4: Wave spectrum changes test 1331